Our cells engage in protein production, and many of those proteins

are enzymes responsible for the chemistry of life.

~Randy Schekman

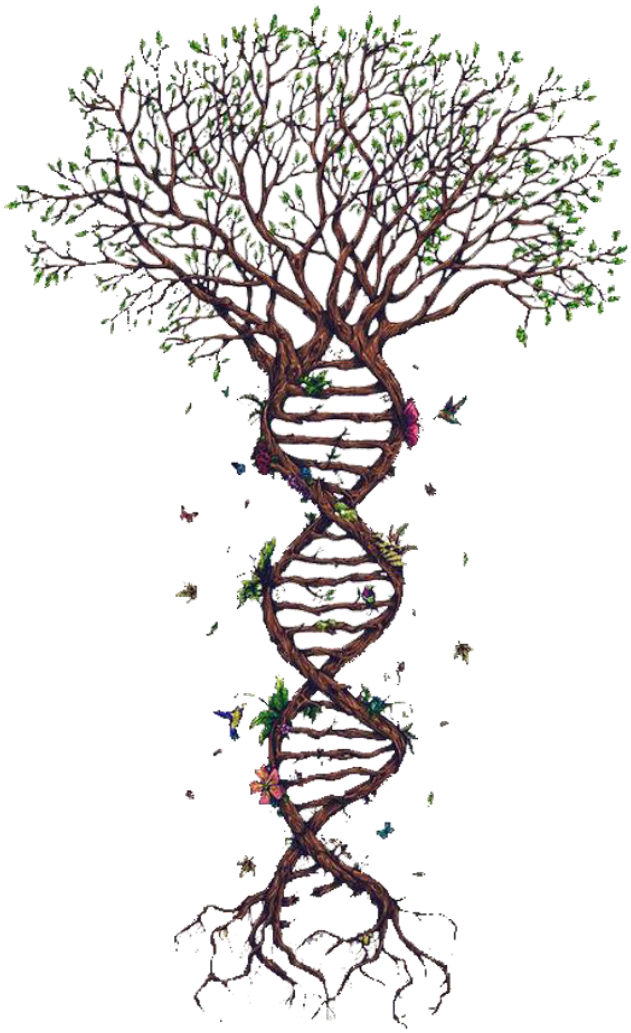

Disclaimer: This was realised with the EEA Financial Mechanism 2014-2021 financial support. Its content (text, photos, videos) does not reflect the official opinion of the Programme Operator, the National Contact Point and the Financial Mechanism Office. Responsibility for the information and views expressed therein lies entirely with the author(s).

CONTENT

INTRODUCTION

The miraculous properties of the milk thistle have been made popular by the herbalist Discorides since the time of ancient Greece. He wrote that the tea of milk thistle seeds could annihilate the poison from the venomous snake bite. Pliney The Elder promoted that a mixture of plant juice and honey helps the gallbladder. It was in 1534 that the milk thistle began to be given as treatment for liver disease by Otto Brunfels. In the late sixteenth century, Culpepper claimed that the plant infusions are excellent for obstructions of the liver and the spleen and also curative for jaundice and for breaking and expelling stones. Rademacher popularized the ethanol extract from the seeds for hepatosplenic disorders [1].

Over the past 25 years, the herbal industry of the U.S. exploded due to the increased interest of the population for herbal products and remedies. In 1994, the Congress of the Dietary Supplement Health and Education Act classified vitamins, minerals and herbs as dietary supplements rather than drugs thus leaving the Food and Drug Administration without too much power over their manufacturing protocols. Since then, the natural remedies market has registered huge profits [1].

Silymarin is a natural supplement and besides this, it has extraordinary medicinal properties, whereas it is included in many phytochemical products. Its functionalization with hydrocarbon radicals in the active hydroxyl positions could give compounds with much higher affinity for lipophilic media. On one hand, these compounds introduced into creams or cosmetics products may overcome the skin's barrier and may exhibit preventive effects on tissue degeneration. On the other hand, they may be included in capsules and pills intended for oral administration, in order to metabolize and to reach the affected target much more easily. The study of the following pages engaged silybin, the main component of silymarin, and various fatty acids into a desired esterification process mediated by cold-active lipases as enzyme biocatalysts. As the extension to uses is traced down above, the novelty element stays beyond the biocatalyst material produced strating from a particular cold-adapted bacterial strain and adjusted up to immobilized protein networks.

GRAPHICAL ABSTRACT

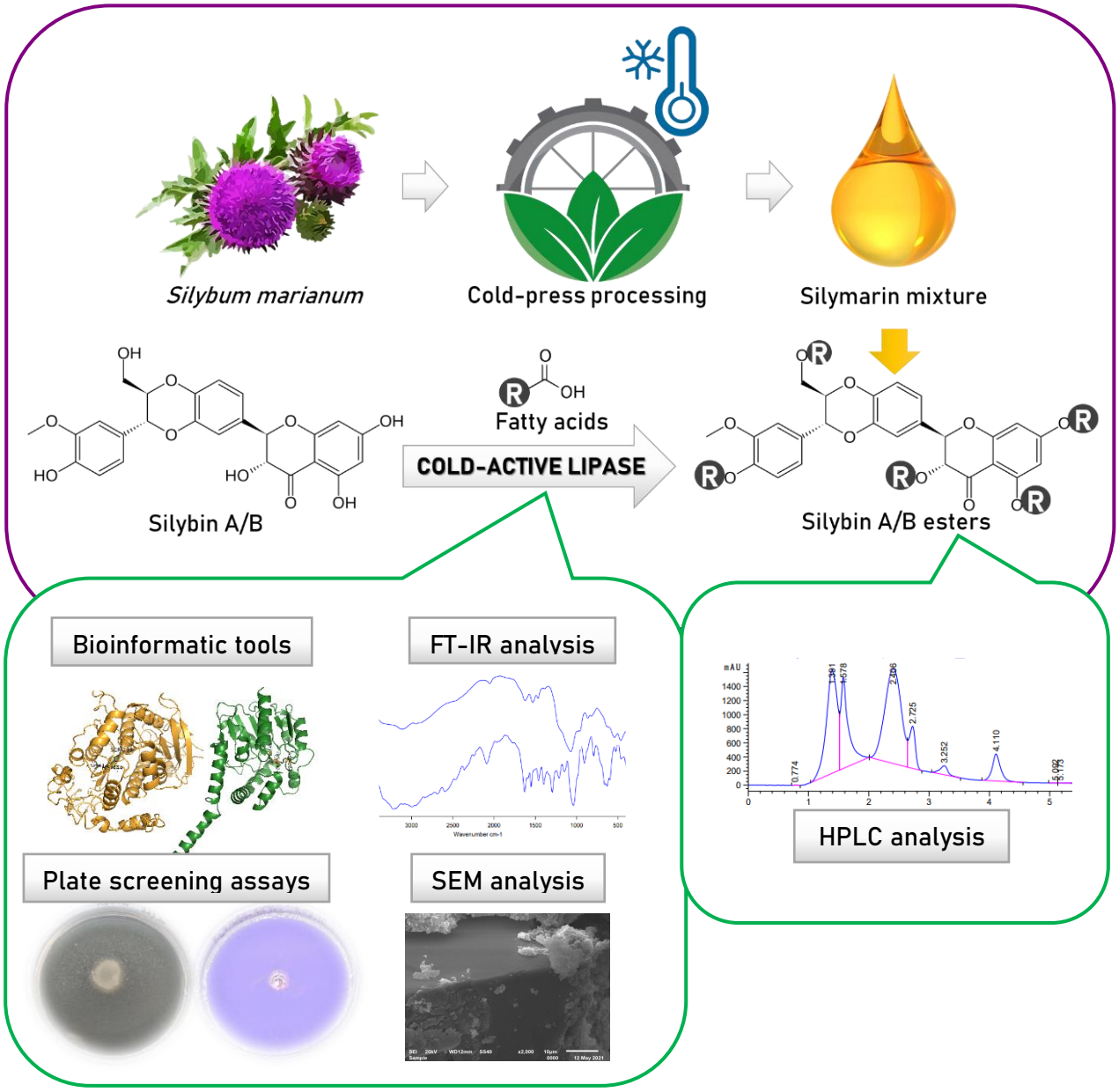

THEORETICAL OVERVIEW

I.Silymarin and its constituents

I.1. Silybin and flavonolignan relatives

Silybum marianum is a very effective natural remedy which has been used since the ancient times, known in the popular consciousness as the milk thistle. It originates from Southern and Southeastern Europe, but due to the multiple colonization of the past, the milk thistle was also spread in the warm areas of America, Asia and Australia along with its medicinal benefits and applications. *Thistle* is the common name of a group of flowering plants characterized by spiked leaves with white veins from which the milk is extracted. *Silybum marianum* belongs to the aster family, *Asteraceae* or *Compositae*, as it could be found in daisies, artichokes and thistles. Reaching the maturity, the thistle plant blooms with a large, purple flower, while its spikes extend to the stem. In a heraldic direction, it is interesting to mention that the crowned thistle is the national emblem as well as a high chivalric order of Scotland since 1249 and also, the official symbol of the city of Nancy, the former capital of the Duchy of Lorraine [1].

From the biochemical point of view, *Silybum marianum* consists of a group of flavonolignans colectively known as the silymarin mixture. Highest concentrations of silymarin are found in the fruit, pericarp, seeds and leaves of the thistle plant with a range of 1.5%-3.5% flavonolignans in relation to the fruit weight [2].

In other words, silymarin comprises silydianin, silychristine and silybin, being noticed that the last compound shows more active biological properties. They fairly act as free radical scavengers and stabilizers of plasma membranes. Silymarin preparations for clinical use became officially adopted in 1969 [1], which has so far trigered an avalanche of studies on its flavonolignan components that induce hepatoprotective effects, as well as antioxidative, antiinflammatory, hypolipidemic and neuroprotective effects [2].

Nowadays, the term silymarin refers to the extract of *S.marianum* from milk thistle which is rich in flavonolignan compounds. European Pharmacopeia claims that milk thistle extract contains 30% to 65% silymarin corresponding to 20-45% silydianin, 40-65% silybin A and B, 10-20% isosilybin A and B. From a chemical point of view, flavonolignans are natural polyphenols, biogenetically related to lignans due to their similar synthetic pathways [3]. They consist of two phenylpropanoid units linked to another complex structural part that ensures the binding of the C_6C_3 ring with that of the flavonoid nucleus in different positions. Due to their extended and complicated structure, these compounds show multiple chirality which leads to the existence in nature of several

stereisomers. The first known source of flavonolignans was isolated 2000 years ago from milk thistle and as a consequence of multiple chirality, *S.marianum* contains 23 natural related components [4].

As previously noticed, silymarin is maily composed of individual flavonolignans and the flavonoid taxifolin. The chemical composition analyzed by HPLC-MS [5] could be studied from the following table (Tabel 1).

Silybin is the main component of silymarin and hence the most biologically active. Structurally, the chromone ring is responsible for the weak acidic properties and the antioxidant response is given by the phenolic hydroxyls from 3,4- and 4,5- suitable positions for the formation of complexes with various metal ions. Very low water solubility (430 mg/L) restricts its therapeutic efficacy even if it is clinically safe at high doses (>1500 mg/day for humans) [6]. Silybin exists in two stereisomeric forms A (2R, 3R, 10R, 11R) and B (2R, 3R, 10S, 11S) having reduced solubility both in water and in lipid medium [7]. All silymarin components' structures are outlined in the figure below (Figure 1).

Tabel 1. Characterization of silymarin mixture by HPLC-MS [5].

Compound	Retention Time (min)	Content (%)
SB A	6,41	16,34+/-1,60
SB B	6,99	21,64+/-1,53
ISB A	8,15	5,73+/-1,16
ISB B	8,44	2,90+/-0,65
SC A	3,1	13,73+/-1,20
SC B	3,82	1,83+/-0,15
SD	3,68	4,55+/-0,62
DHSB	12,47	0,33+/-0,07
DHSC	8,02	0,56+/-0,09
TA	1,99	2,09+/-0,41

In this direction there are many semisynthetic modifications to increase the bioavailability while retaining its biological activity. It is the case of Legalon®, a common drug intended for liver therapy, which contains bis-hemisuccinate derivated silybin with high affinity for aqueous environment. There are also other modifications in order to increase the solubility in water, such as phosphodiesterification and glyco-conjugation. At the opposite pole, silybin derived at 7-OH group with palmitate or at 23-OH with acyl residues tends towards hydrophobic media [7]. Otherwise the structural modifications are imperious because silybin undergoes intensive Phase II metabolism and is rapidly excreted in bile and urine, leading to low therapeutic efficacy. By all means, oral administration of the drug is preferred, although in the case of silymarin extracts only 9 ng/mL concentrations are absorbed into plasma. When an active agent is orally delivered, it must first

dissolve in gastric and/or intestinal fluids in order to permeate the membranes of the gastrointestinal tract to reach systemic circulation [8].

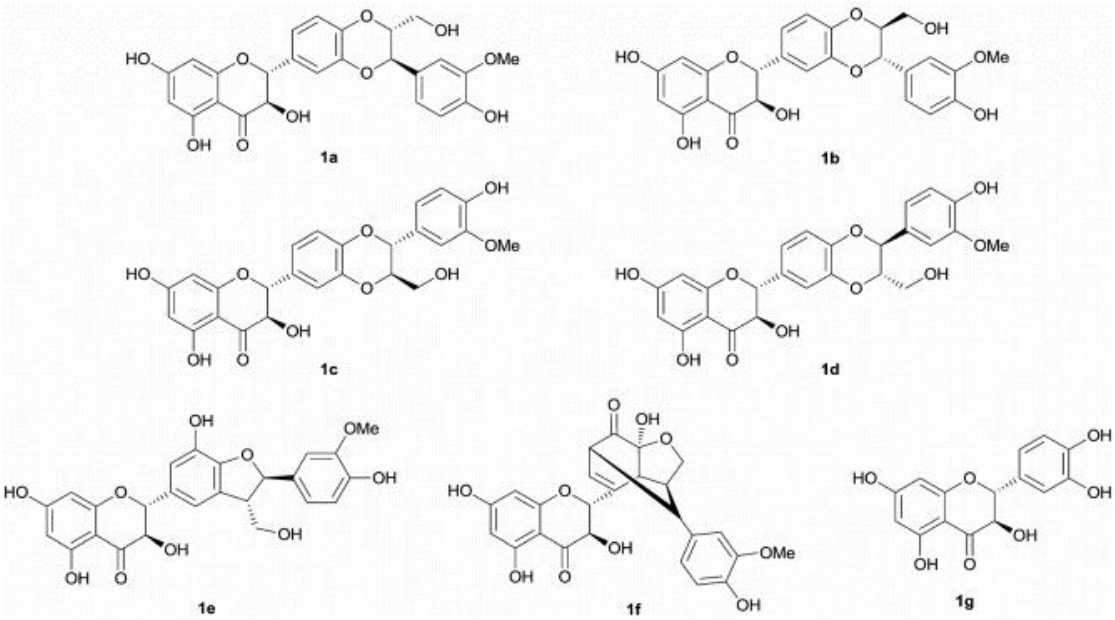

Figure 1. Structures of silymarin components: (1a)-silybin A, (1b)-silybin B, (1c)-isosilybin A, (1d)-isosilybin B, (1e)-silychristin A, (1f)-silydianin, (1g)-taxifolin.

I.2. Medicinal benefits of silymarin

In the last decades, many hypotheses and studies on the miraculous properties of silybin and silymarin have been stated. Silybin functions primarily as an antioxidant therefore this term must be correctly understood. Generally, antioxidants exert protective effects on the biomolecules and biocomponents which are subjected to oxidative stress. In the living organisms antioxidants associate themselves in complex biological systems, often as redox tandems in order to prevent and repair proteins, lipids and nucleotides from damage caused by reactive oxygen species (ROS, e.g., OH• , O_3 •, NO, ROO•, H_2O_2, $^1O_2$, HClO, etc). Being inductory of oxidative stress, ROS are a cause of autoimmune diseases through the interaction between the intact and the damaged proteins, involving the so-called cross-immune reactivity [9]. It has to be mentioned that at larger concentrations, antioxidants could also become harmful oxidative stressors. The most important antioxidants are undoubtedly the vitamins (ascorbate, retinol and tocopherol), carotenoids and flavonoids. Recent studies revealed that antioxidants could also play the role of mediators for some nuclear receptors engaged in the production of intracellular enzymatic antioxidant systems. The combination of various antioxidants results in the formation of hybrids with a pronounced antioxidant effect. There are useful exemples described in the literature: tocopherol and procaine, flavonolignans and fatty acids, improved ascorbic acid, iron chelator deferiprone [10].

In the recent past, silymarin started to be introduced in dermatological and cosmetic preparations for its antioxidant effect and its capacity to withstand the UVB- and chemically- induced damages. There are various factors, both intrinsic (genetic) and extrinsic (environmental), leading to a perpetual process of functional and structural modifications in skin tissue. Solar radiation caused by UV (295-400 nm) wavelengths reaches the earth surface and initiates skin reactions that result in reactive oxygen species formation (ROS). These free radicals drive to carbonylated proteins, peroxidated lipids and enzyme activation, thus causing the remodeling of the extracellular matrix. It is the first signal of collagen and elastan fibers destruction, of lowering the skin hydration and increasing the inflammatory susceptibility. Collagenase and elastase hydrolyze the support and integration networks of skin tissue, breaking down collagen and elastic fibers. Moreover, hyaluronidases section the hyaluronic acid into smaller fragments, influencing the hydration capacity of the skin [5].

As a consequence of the antioxidative effect proposed by silybin, a number of other properties related to the antioxidative ones could be formulated. Reported activities include inhibition of lipid peroxidation of hepatocyte, microsomal and erythrocyte membranes in rats, and protection against genomic damages by suppression of hydrogen peroxide and super oxide anions and of lipoxygenase. It is considered that silybin also influences hepatocyte synthesis by stimulating the activity of ribosomal RNA polymerase, as well as protecting against radiation-induced suppression of hepatic and splenic DNA and RNA synthesis [1]. Silymarin with anti-oxidative, anti-fibrotic, antiinflammatory, membrane stabilizing, immunomodulatory and liver regenerating properties plays an important role in experimental liver diseases. There are also significant responses of flavonolignans to mushroom (*Amanita sp.*) poisoning, hepatitis, cirrhosis and liver fibrosis [3]. Moreover, silymarin increases the activity of anti-oxidant enzymes like superoxide dismutase, catalase, gluthatione peroxidase, gluthatione reductase and gluthatione-S transferase. The molecular mechanism of the antioxidant activity is based on the functions of each hydroxyl groups, these offering the suitable positions for silybin derivatization without losing the biological activity of the resulting conjugates [8].

Silymarin inhibits all stages of carcinogenesis, acting as a prophylactic and therapeutic agent in the treatment of more advanced and agressive forms of cancer. It is highly recommended for effective control of chemotherapy and radiotherapy-induced toxicity by inhibiting the expression and the secretion of the growth factors that cause the formation of the tumor cell lines [8].

1.3. Silymarin extraction from natural sources

Freudenberg was the first who built the hypothesis of naturally biosynthetical processes in formation of flavonolignans in *S. marianum* (purple flowering plant): starting from (+)-taxifolin and coniferyl alcohol in an oxidative environment provided for peroxidase enzyme catalytic activity. Firstly, there are formed neutral phenoxy and quinone methide radicals, followed by O-coupling. Finally, a thermodynamically controlled nucleophilic attack of the hydroxyl group on the quinone methide system through an intermediate affords the 2,3-trans-substituted 1,4-benzodioxane skeleton. The production of flavonolignans in the white-flowered variant is different, whereas instead of taxifolin, the 3-deoxy derivative eriodictyolmay is involved in the biosynthesis [3].

Synthetically, silymarin is extracted from *S. marianum* fruits with amphipolar solvents methanol, 80% methanol, ethanol and ethyl acetate by percolation or with the use of Soxhlet apparatus. The fatty materials from the fruit extract are removed by extraction with n-hexane or petroleum ether, beining obtained flavonolignan-containing extracts. Typically, the seeds of *S.marianum* are partially defatted by pressing, which lowers the fat content from approximately 25 to 8 %. Then the seeds are extracted with acetone (alternatively ethanol, methanol or ethyl acetate). Acetone extract is partially evaporated and the remaining fat is removed by hexane extraction. Crude silymarin (complex) precipitates after further evaporation. Pure silybin is prepared by dissolving silymarin in absolute ethanol followed by addition of about 10 % water. Crude silybin, which precipitates could be further purified by recrystallization from ethanol [8].

At industrial level, the extraction of silymarin is performed with ethyl acetate and acetone. Further, silymarin components are separated by solvent-solvent partition and different chromatographic techniques such as OCC, TLC, LPLC, RP- and NP-MPLC, RP- and NP-HPLC. The separation of diastereoisomers of silybin, isosilybin and silychristin and regioisomers (−)-silandrin and (−)-isosilandrin was accomplished in the 2000s by RP-HPLC, MPLC and HPLC. Moreover, the isolation process of the extracted fractions was monitored by analytical TLC or HPLC [3].

A greener method of extracting the silymarin mixture from the milk thistle proposes the use of water that solubilizes natural compounds at high temperature and elavated pressure. Give the physical parameters: dielectric constant, surface tension and viscosity of the water, which all are absolutely dependent on the temperature, adjusting the temperature and the pressure could bring the water in a strong solvent stage with similar properties to organic solvents. Unlikely organic solvents, which require defatting of the milk thistle prior to extraction, water extraction did not require deffating. This procedure assumes that 0.5 g of milk thistle seeds are milled to an average diameter of 0.4 mm and then introduce into the extraction cell along with 2 g of washed sea sand. The cell is installed in the GC oven and the water starts pumping into the cell with a constant flow. The pressure

is maintained above the water pressure at the desired temperature of 140°C. After collectinng the fractions at well-defined time intervals, 1 mL of each sample is subjected to compressed nitrogen drying, then redissolved in methanol, filtered and analyzed by HPLC. The results could be observed in the next table (Tabel 2) [11].

Tabel 2. The efficiency of flavonolignan extraction by hot water procedure [11].

	Maximum yield (mg / g seed)			
Temperature(°C)	**Taxifolin**	**Silychristin**	**Silybinin A**	**Silybinin B**
100	0,6	2,3	1	1,6
120	0,7	2,5	1,2	2,2
140	0,5	2,4	1,2	2

Cold press method is proposed by Derya Duran et al. as being a more economical technique compared to solvent extraction and hot press along with its simplicity and energy efficiency. It has been reported to be the best way to produce high-quality oil. The popularity of the method increased since no heat or chemical treatment is used during the cold press process and all beneficial nutritional properties of the raw material are transmitted to the oils. These oils consist of natural phytochemicals as tocopherols, fatty acids, sterols and antioxidant phenolic compounds. However, after the cold press method two fractions are obtained: the oil and the waste and silymarin is completely passed into the residue, so the problem arises in the light of the valorization of biomass waste [2].

I.4. Improvement of silymarin properties

It is undeniable that nowadays silymarin is a popular medicine due to its hepatoprotective, antioxidant, antiviral and antitumoral properties, but there are also some drawbacks concerning its water solubility, poor intestinal absorption as well as an elavated metabolism for each of its flavonolignan components [12]. In this direction studies have been carried out in order to increase the bioavailability of silymarin by developing new drug designs. These include drug modifications such as salts, esters and complexes with hidrophilic excipients, complexation reactions with cyclodextrines and phospholipid, formation of biocompatible polymer dispersions, lipid-based delivery systems, nanoemulsions and encapsulation in biodegradable nanomaterials [6].

In the main area of pharmacological interest stays the self-emulsifying drug delivery technique through which amphiphilic particles are formed, with the drug inside a surfactant molecules coat. The gastrointestinal absorption is greatly facilitated due to the surface interactions of these amphiphilic systems. The supersaturation of these systems could drive a faster absorption but thermodinamically, it is an unstable state that tends to return to the equilibrium by drug precipitation. This inconvinient

can be overcome by precipitation inhibitors such as amorphous solid dispersions with PVP and PVA polymers [12]. The following figure outlines several methods by which the higher bioavailability of silymarine could be obtained (Figure 2).

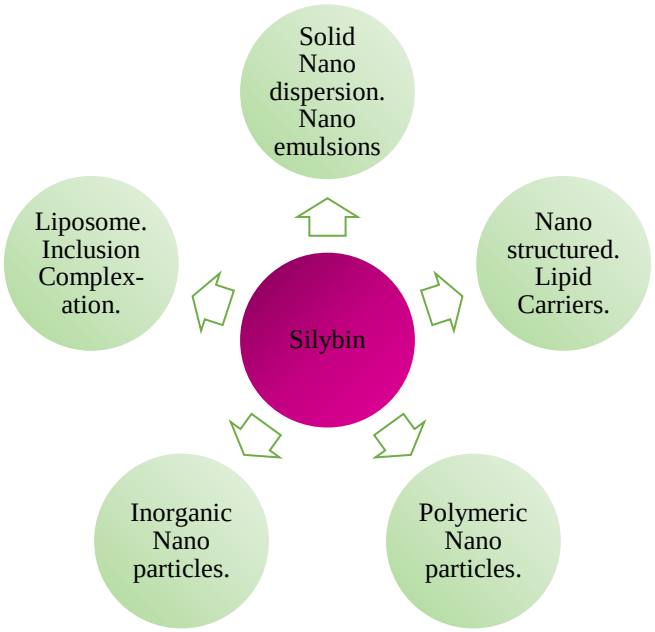

Figure 2. Silybin modification methods.

A demonstrative study of the bioavailability improvement is given to the scientific community by S. Drouet et al. which achieved a selective acylation of silybin in 3-OH position to give 3-O-palmitoyl-silybin in the presence of Lewis acid $CeCl_3 \cdot 7H_2O$ as it could be oserved in the Figure 3. The yield reached was around 60%, with 85% of palmitate linked in position 3-OH and 15% in position 5-OH but with no negative change in antioxidant capacity of the derivative [7].

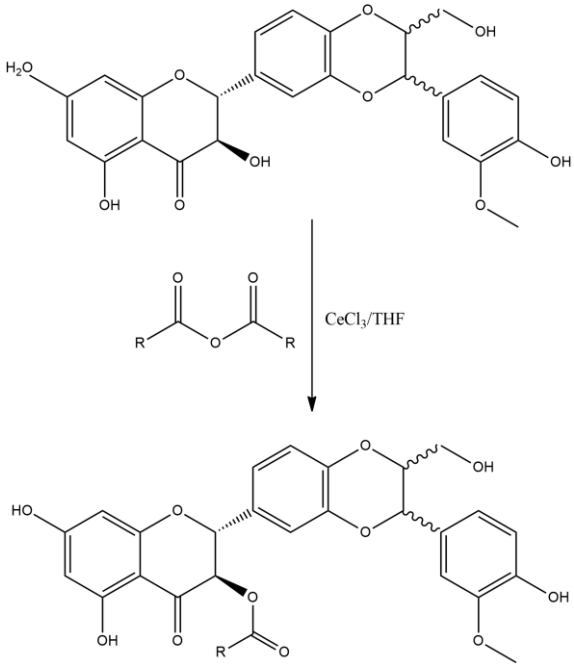

Figure 3. 3-O-palmitoyl-silybin synthesis

Two methods of radical scavenging were performed to demonstrate this: ferric reducing antioxidant power (FRAP) used for hydrophilic antioxidants, and copper reducing antioxidant capacity (CUPRAC) used for lipophilic and hydrophilic antioxidants. With FRAP assay the radical scavenging of silybin was 1.74 times more effective than give 3-O-palmitoyl-silybin while the derivative was 1.55 times more effective than silybin with the CUPRAC assay [7].

Besides the chemical modification methods, there are encapsulation variants of the compound of interest in matrices much better accepted by the organism. In the following are outlined some models. Silymarin could be included in natural β-cyclodextrines forming complexes often used because of their solubilization potential in the body barriers and of their preventive effect on metabolic degradation [6]. Other types of molecular complexes capable to enhance the bioavailability of the active constituents of silymarin are represented by phytophospholipid complexes known as phytosomes. The phytosome unit is a molecular complex between phospholipids and standardized polyphenolic constituents in a 1:1 or 2:1 molar ratios. The literature promotes the silybin-phytosome system as having a more intense therapeutic activity compared to that of the unmodified compound [12]. Further, liposomes are hollow spherical nanoparticles with a closed shell of a lipid membrane (mono- or multi-layer), inside of which an aqueous solution can be encapsulated. These supramolecular aggregates owe their success as carriers of therapeutic drugs for many advantages including the capability to encapsulate both hydrophilic and lipophilic drugs, having targeting and controlled release properties, cell affinity, tissue compatibility, reduced drug toxicity and improved drug stability. Moreover, liposomal systems are known to find an immediate access to the reticulo-endothelial system (RES) rich sites like liver and spleen, and this self-targeted nature of liposomal carriers can be exploited well for drug distribution to hepatic site. Thus being said, flavonolignan components of silymarin could be integrated into liposomal systems in order to increase their properties [6].

II. The cold-active enzymes

II.1. Concept

The biotechnology is highly promoted because it is environmentally friendly and has a valuable potential to take the place of the chemical industry based on the petrochemical refineries, which use harsh reaction conditions. With the interest of the scientific world focused on renewable resources and Green Chemistry, the bio-catalytic approach becomes highly appreciated in the new generation of synthetic processes, where chemicals of industrial value are obtained under mild conditions from renewable sources of biomass, in most cases [13]. Chemical syntheses based on

enzymes used as biocatalysts are topical because of the reduction of the number of synthesis stages, high efficiency of atoms, by avoiding the protection steps [14], to a good regio- / enantio-type selectivity, which could be achieved under mild process conditions, in other words, green conditions. New bio-catalytic concepts have been launched using enzymes, either solubilized in the reaction medium (homogeneous bio-catalysis) or immobilized (heterogeneous bio-catalysis) [15].

This study brings in the spotlight the enzymes from organisms that live in extremely harsh environmental conditions, which to some extent simulate the conditions available in industrial processes. Extremophile microorganisms that live in cold environments represent a particularly interesting source of living material adapted to abnormal conditions or considered extreme in comparison to those confortable for human beings [16]. In contrast, organisms that live in moderate environmental conditions may be termed mesophiles or neutrophiles. As previously mentioned, microrganisms that adapted and colonized cold places on Earth may be divided into psychrophilic or psychrotolerant depending on the optimal temperature of development. Psychrophilic organisms grow onto significant low temperature range between -20 and 10°C being although unable to develop at temperatures higher than 15°C. Meanwhile, psychrotolerants optimally grow between 20 – 25°C and even register high metabolic activiy at values below 0°C. This behavior could be explained by the fact that psychrophiles are usually found in marine ecosystems while psychrotolerants thrive in terrestrial cold environments.These cold-adapted microorganisms mostly include bacteria, yeasts, fungi and algae. Cold and frozen areas of the terrestrial biosphere include polar circles (Arctic and Antarctic), deep water and frozen altitudes of mountains along with glaciers, ice sheets and permafrost [17]. As a general information, the temperature recorded annually at the poles is always below zero degrees, and during the winter, the thermometers reach -80°C [16]. The polar regions represent 15% and the permafrost 20% of the total surface of the Earth, while the microorganisms able to maintain their life throughout the geological evolution of these platforms are of psychrotolerant type. The aquatic surface of the Earth represents 75% with an average temperature of 3°C, but it is extraordinary to be notified that at the bottom of the seas and oceans the micro-organisms of psychrophilic type coexist and develop in the absence of light, at high pressures and without valid food. At the level of glaciers, they develop in the wires and films of liquid that spread over the mineral grains to ensure their nutrient needs [16].

II.2. Diversity of cold-active enzymes

Microorganisms inhabiting low-temperature environments have been adapted in order to survive by the production of cold-active enzymes to ensure the minimum rate of chemical and metabolic reactions and of ice-binding proteins, designed to control the growth of ice crystals thus

combating frost and membrane rigidity. Usually, the optimum temperatures for the activity of the cold-adapted enzymes are in the range of 20 – 30°C, which can be considered close to that of the thermophiles. The ability of these enzymes to incorporate a significant fraction of their activity at low temperatures is based on their structural flexibility. It is worth mentioning that an increase in the flexibility of the enzyme is not necessarily proportional to the decrease in their thermo-stability. There are two strengths related to the active enzymes operating, one of them is for the manipulation of thermo-labile and sensitive substrates at low temperatures and the other facilitates the inactivation of the enzyme as the temperature increases [17].

One aspect that may be less well known is that microorganisms that live in very cold areas, somehow avoid frost, rather than fight it. This contribution is due exclusively to proteins that mediate the binding capacity of ice crystals. The ice-binding proteins are adsorbed on the ice surface leading simultaneously to the decrease of the freezing point and to the slight increase of the melting point of water. This dependence could be clearly observed following the analysis of thermal hysteresis, whose width correlates with the concentration and functions of the protein [18].

Moreover, the adsorption of proteins on the ice crystals leads to their stabilization and inhibition of the recrystallization process. Indeed, ice recrystallization inhibition is of utmost relevance in all freezing processes involving living cells and food products, since large ice crystals damage cell membranes and impair cell viability and food quality [18].

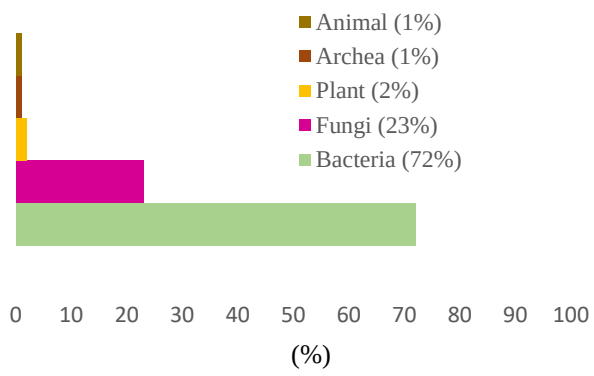

Figure 4. Organism sources of cold-active lipases

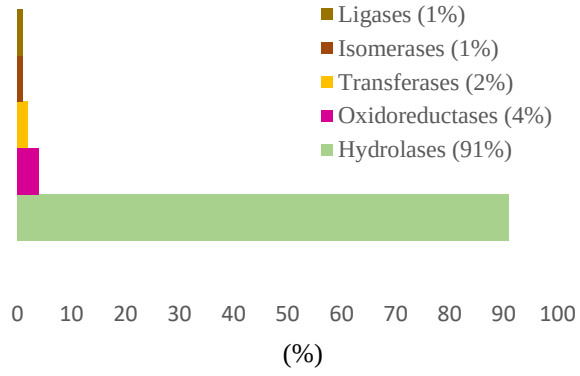

Figure 5. Distribution of cold-active enzymes based on enzyme classes

The majority of cold-adapted enzymes have been expressed in heterologous hosts being obtained from psychrophilic and psychrotolerant microorganisms, bacteria or fungi as it could be observed in Figure 4. Distribution of cold-active enzymes based on enzyme classes could be analyzed in Figure 5. To perform catalysis at low temperature demands high flexibility for proteins that adversely alters the stability of the enzyme. However, there are very interesting examples of enzymes

with high thermostability, as is the case of the superoxide dismutase, DaSOD, isolated from a psychrophilic organism, *Deschampsia antarctica*, whose optimum temperature is 20°C but it records a catalytic response even at -20°C. At 0 degrees it retains up to 80% of its catalytic activity [16].

Most of the time, the catalytic properties of mesophilic organisms at reduced temperatures are unusual, as is the case of *Candida albicans* lipase, with an optimal temperature of 15°C or *Arabidopsi* β-amylase 3 with great residual activity at low temperatures. More surprising is to discover a thermophilic enzyme with high activity at low temperatures. For instance, β-galactosidase isolated from *Pyrococcus furiosus* has optimal activity at 90°C, but retaining 8% of its activity at 0 degrees. Comparatively, the lactase activity of *P. furiosus* at 0°C was still 40% of the optimal activity from the main β-galactosidase use in the food industry (28 U/mg at 50°C and pH 7.0) from *K. marxianus*. In addition, the lactase activity of *P. furiosus* at 0°C was 31% of the optimal activity of a cold-active β-galactosidase from *Arthrobacter psychrolactophilus* strain F2 (33 U/mg at 10◦C and pH 8.0) [16].

II.3. Gene cloning and protein engineering

The most convenient method to discover, even create new enzymes refers to the expression of protein chains in different cell and microbial cultures. Many studies have revealed the heterologous hosts used for the expression of cold-active enzymes as it could be observed in Figure 6. From the existence of microbial diversity, only a minor fraction can be reproduced through laboratory experiments in human handling conditions. Extremophile microorganisms depend upon drastic conditions to grow and reproduce, nonetheless, cloning techniques suppress the obstacle by various methods [17]. Metagenomics is the main culture-independent approach involving DNA extraction from the environmental sample, isolation of targeted genes and cloning the material further to create a genomic library. Novel enzymes could also be assembled by computational genomics using available information in genome databases without the need of a natural sample. The discovery of novel cold-adapted enzymes is a real challenge, because only a few genomes of psychrophiles have been deposited in public databases [19].

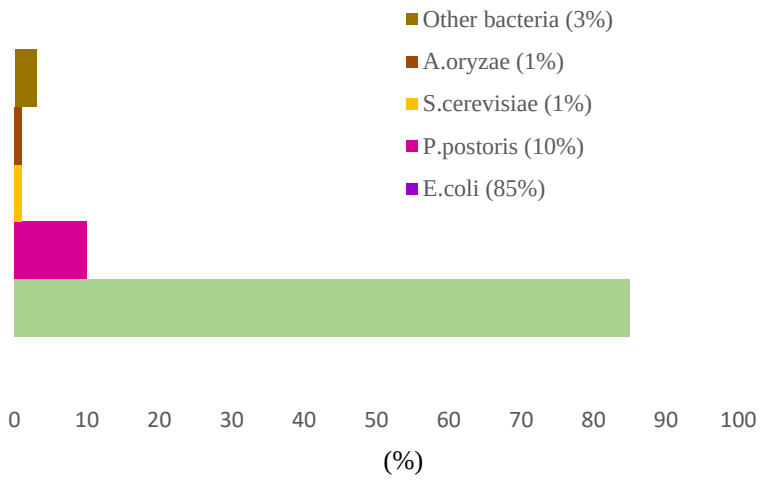

Figure 6. Distribution of heterologous hosts used in the expression of cold-active enzymes

The first step is the isolation of the adapted microorganism, which stands out with good enzymatic activity. The main cloning method is based on the creation of specific primers for gene amplification that uses a DNA strand as a template [19]. This method is possible if the genome of the species is completely sequenced and stored in the gene bank, so the microorganism can be cultivated. There are several valid hosts for gene expression, but *E. coli* is the most popular in this case. Various genotypes have been used but the preferred strain is BL21. Nevertheless, other expression hosts have been researched, such as *Halobacterium* sp. for the expression of a cold-adapted hydrolase, and *Pichia pastoris*, used as the expression host for 9 proteins including various fungal enzymes. Half of the adapted genes were cloned into pET vectors and only 5 were integrated into pCold plasmids. The enzyme purification process often calls for His tag fusion while optimal temperature is an important parameter of enzyme characterization as a result of their complete or partial adaptation to cold [16]. By far the most preferred cold-active enzymes are from the hydrolase class, more specifically lipases and esterases. This concentrates all the research efforts on solving their three-dimensional protein structure. Several strategies have been suggested to promote proper expression and folding of cold-active enzymes expressed in heterologous host, increasing their solubility, activity, and yield [19].

II.4. Applications of cold-active enzymes

Introduction of cold-adapted enzymes to traditional production schemes actually diminishes the panorama of the energy consumed at each step of the process, which is explainable because no thermal energy is needed, the reaction yields are appreciable, the enzymes retain their stereo-specificity at low temperatures, which excludes secondary reactions. Moreover, their thermal lability at higher values rapidly leads to the inactivation of enzymes, hanging up the process [20].

The ability to heat-inactivate cold-active enzymes has particular relevance to the food industry where it is important to prevent any modification of the original heat-sensitive substrates and products. This is also of benefit in sequential processes (e.g. molecular biology) where the action of an enzyme needs to be terminated before the next process is undertaken, easily by heat-inactivation [20]. Examples of biotechnological applications of enzymes are provided further and the application classes are listed in Figure 7.

Nonetheless, the industrial applications of cold-active enzymes are still in the early stages. As far as concerns the food sector, cold-active amylases (EC 3.2.1.1) are of great interest for baking and brewing products, since they could be easily inactivated during cooking. A patent developed from *Bacillus licheniformis* with Novozymes improved the catalytic activity in a decreased temperature range from 10 to 60°C. Another patent developed with ColdZYMES ApS was used to heterologously express *Clostridium* α-amylase at lower temperatures than 10°C. The cold-active variants are frequently exploited for milk processing or refrigerated storage as is the case of β-D-Galactosidase usage. Among proteases (EC 3.4.) from psychrophilic sources, that from *Pseudoalteromonas* strain SM9913 might be used in tenderizing collagen-rich meat, while that from *Flavobacterium balustinum* promises wider applications, due to its optimal temperature of 40°C and high thermolability (full inactivation at 50 °C in ca. 10 min) [18].

Cold-active enzymes could be used in chemical manufacturing for organic compounds that are highly volatile and can only be modified at low temperature. In other cases, low temperature may make separations of the product easier and less expensive. Cold-active enzymes could be added to detergents for low-temperature washes or to other solutions for cleaners. Some enzymes might replace chemical preservatives in foods by depleting metabolites required by other organisms, disrupting microbial cells, or degrading other enzymes. Psychrophilic microorganisms and their enzymes are already crucial to nutrient cycling and biomass degradation and production. We can take advantage of the natural role of psychrophiles and use ones producing useful enzymes in waste-water treatment, biopulping and bioremediation in cold climates. Psychrophilic methanogens would be useful in anaerobic digestors to increase methane production in Northern regions. In research, reactions could be performed at low temperature and then the mixture heated to readily inactivate the enzyme before proceeding to the next step. Other cold-active enzymes could substitute for currently used enzymes that require higher temperatures than the cells or substrates require [17].

In the field of molecular biology, the enzymes are the main actors. Several *in vitro* reactions necessite low temperature, a condition that could be fulfilled and enhanced by the cold-active enzymes. Ligases (EC 6.5.1.1) catalyse the formation of phosphodiester bonds, joining DNA fragments with protruding or blunt ends. For DNA with protruding ends, the optimal ligation temperature is a compromise between the ligase Topt and the optimal temperature for annealing short

DNA protruding ends, usually very low. For this reason, the reaction efficiency can be increased by low temperatures (4 – 8°C) and by extending the incubation time over several hours. Proteases (EC 3.4.) are used to remove protein contaminants from nucleic acid preparations. The most popular is Proteinase K, which retains relatively high activity at 20°C and is stable up to 95°C [18].

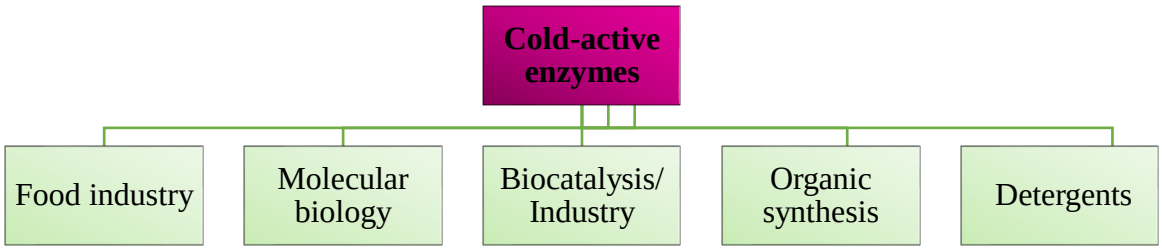

Figure 7. Application classes of cold-active enzymes.

II.5. Lipases vs. Cold-active lipase

Carboxylesterases (EC 3.1.1.1) and true lipases (EC 3.1.1.3) are altogether called lipolytic enzymes. Carboxylesterases (in the following text called esterases) usually act on water-soluble esters, while true lipases (in the following document called lipases) can hydrolyze water-insoluble substrates, too. The longer fatty acid chain in lipid is the less water-soluble it is; therefore, enzymes that hydrolyze olive oil (triglyceride ester with long-chain (C16, C18) fatty acids) are called lipases and those that hydrolyze tributyrin (triglyceride ester with short-chain (C4) fatty acids) are called esterases [21]. Essential characteristics of lipases must to be inserted, for the sake of structural complexity these present [21]

- The active site clefts of these lipases are covered with a flexible and amphiphilic α-helix, which functions as a "lid." Upon binding to the surface of substrate micelles, the lid undergoes structural changes resulting in the displacement of the α-helical lid from the active site cleft. In this so-called "open" conformation, the hydrophobic surface area surrounding the catalytic site increases allowing the four substrates to diffuse into the active site freely. However, interfacial activation cannot be the property distinguishing between esterases and lipases as some lipases do not follow interfacial activation kinetics.
- Despite low amino acid sequence similarity among lipolytic enzymes, being very often even below 20%, most of them share a conserved α/β-hydrolase fold and a canonical GXSXG-pentapeptide around the catalytic serine. Later, a second sizeable structural family of lipolytic enzymes with a GDSL catalytic site consensus motif and an α/β/α-fold was discovered. Presently, only a few lipolytic enzymes with a β-lactamase like fold structurally unrelated to α/β- and α/β/α-hydrolases were found.

- The canonical α/β-hydrolase fold is characterized by a central hydrophobic sheet composed of eight β-strands with the second one mostly antiparallel. The strands β3 to β8 are connected by α-helical-loop structures organized at both sides of the sheet. This stable globular scaffold is characterized by extraordinary plasticity as different structural elements and even whole domains, e.g., the above mentioned "lid" or "cap" described for many lipases, can be inserted into these loops connecting β-strands and α-helices without disturbing the fold itself.
- The active sites of lipolytic enzymes contain a catalytic triad consisting of a strictly conserved nucleophilic serine and histidine and an aspartate or glutamate as acidic residues. The catalytic serine is usually embedded within the conserved motif Sm-X-Ser-X-Sm, where "X" and "Sm" denote any amino acid and small amino acid, respectively. For most lipolytic enzymes, a GXSXG-consensus motif located in the middle of the sequence was reported. Glycine residues of the GXSXG-pentapeptide account for the localization of the catalytic serine on the top of a sharp turn preceded by an α-helix and followed by a β-strand. This structural motif, named "nucleophilic elbow," seems to be a steric prerequisite for substrate hydrolysis and represents one of the best conserved structural motifs among α/β-hydrolases.
- The catalytic cycle of serine hydrolases involves deprotonation of the side chain hydroxyl group of serine by a catalytic triad histidine, which is deprotonated by the acidic residue. The deprotonated serine initiates the hydrolysis of an ester bond by a nucleophilic attack on the carbonyl carbon atom of the ester substrate. After the corresponding alcohol is released, a lipase–acyl complex is formed, which is subsequently hydrolyzed by water releasing the free fatty acid and the enzyme. During the hydrolysis, the negatively charged intermediates with the tetrahedral configuration at the oxygen atom of the ester bond are stabilized by the so-called oxyanion hole (mostly formed by asparagine and glycine) varying in type but structurally strictly conserved among α/β-hydrolases.
- The canonical α/β/α-hydrolase fold of the GDSL family of lipolytic enzymes is characterized by a conserved hydrophobic core consisting of five β-strands and at least four α-helices. The additional secondary structural elements and differences in the substrate-binding loops inserted in the canonical α/β/α-fold are the cause of functional diversity among GDSL hydrolases. This is reflected by the broad spectrum of substrates hydrolyzed by these enzymes, including glycol esters, aryl esters, wax-like lipids, phospholipids, lysophospholipids, acyl-CoA thioesters, peptides, and triacylglycerols.
- The GDSL-motif containing the active-site serine residue is part of a consensus sequence designated as block I, which is positioned close to the N-terminus of the enzyme. The catalytic triad residues, namely aspartate and histidine, were identified in blocks III and V, respectively. The glycine belonging to the oxyanion hole is a strongly conserved residue of block II. This

observation led to the proposal of the new name SGNH-hydrolase family that is now used as a synonym to the GDSL-hydrolase family. Different from α/β-hydrolases, the catalytic histidine and aspartate are part of a DXXH-motif. Furthermore, the nucleophilic elbow strongly conserved among α/β-hydrolases is absent in GDSL-hydrolases. Despite notable differences, the GDSL-hydrolase catalytic mechanism is similar to the general mechanism of α/β-hydrolases, which all have a Ser-His-Asp catalytic triad.

Up to date, lipolytic enzymes are classified into nineteen families based on phylogenetic criteria, conserved sequence motifs, and biological functions. For this particular study, there have been identified two lipases out of the proteome of *Psychrobacter* sp. of Scarisoara Ice Cave (Romania), as belonging to the fourth and fifth family of lipases.

Family IV of lipases constitutes several esterases from distantly related prokaryotes, including psychrophilic, mesophilic, and thermophilic bacteria. The enzymes show a remarkable similarity to the family of mammalian hormone-sensitive lipases (HSL). Here, three sequence blocks with conserved motifs were identified, with blocks II and III containing the catalytic triad residues. Block I contain a conserved HGGG consensus sequence that is involved in hydrogen bonding interactions, which stabilize the oxyanion hole and promote catalysis as deduced from the crystal structure of *Brefeldin A* esterase from *Bacillus subtilis* [21].

Despite their homology to HSL, the substrate spectra of the enzymes of the bacterial HSL-family differ significantly. While human HSL has a broad substrate specificity and hydrolyzes short-chain esters as well as water-insoluble substrates like trioctanoin, vinyl laurate, and olive oil, the bacterial HSL-family esterases show activity only towards short fatty acid chains length substrates like tributyrin and vinyl propionate. Moreover, esterase enzyme kinetics was observed, while HSL reactions show typical lipase kinetics.

Several family IV esterase structures, among them, thermostable esterase from *Alicyclobacillus acidocaldarius* (AaEst), were solved, which showed a unique structural feature: a “cap” which differs from the lid found in true lipases is formed by two separate helical regions and covers the active site. More recently, an oxadiazole inhibitor was identified, which covalently binds to the catalytically active serine. Interestingly, inhibition was specific in that the activity of other carboxylesterases was not affected, providing a promising option for quick discrimination among esterases.

From *Familly V of lipases* [22], esterases originate from different bacterial genera representing mesophilic, cold-, or heat-adapted organisms as *Pseudomonas, Haemophilus,* and *Moraxella*. These enzymes share significant homology with other bacterial proteins like epoxide hydrolases, dehalogenases, and haloperoxidases that also possess the typical α/β-hydrolase fold.

Conserved amino acids are located in three blocks with the catalytic triad residues Ser located in block II, Asp, and His in block III. The esterases Est2 of *Acetobacter pasteurinanus* and EstV of *Helicobacter pylori* are the only enzymes of this family that has been cloned and characterized yet. Both proteins revealed typical characteristics of carboxylesterases with EstV of H. pylori showing a preference for short fatty acid chain lengths, p-nitrophenyl esters (C2–C6), and triglycerides (C4) and typical Michaelis-Menten kinetics instead of interfacial activation. In the case of *A. pasteurianus* Est2, triglyceride substrates with even shorter fatty acid chain lengths like triacetin and tripropionin were hydrolyzed, preferably.

Starring cold-active lipases, extreme organisms develop in a reduced temperature range of 25 and 45°C, due to their adaptation to the inhabiting environment by producing enzymes, along with other biomolecules, which possess specific bio-catalytic activity at low temperatures [23].

Their cold adaptation provides such flexibility around the active sites, along with low enthalpy and affinity towards substrates, but high specific activity at low temperatures. Most of lipases investigated so far have been isolated from psychrophilic and psychrotolerant microorganisms of polar areas, deep water, or chilled food samples. However, these enzymes are slightly thermostable because they have developed in the context of very low temperatures, so the improvement of their thermal stability is obtained by immobilization, directed evolution, protein engineering, chemical treatments. An extremely interesting observation is that the cold-resistant lipases extracted from organisms of tropical areas show very good thermo-stability compared to the analogues of the alpine areas [23].

Like all other lipases, the cold-resistant possess the canonical α/β hydrolase fold (central, hydrophobic β-sheet that is covered by α-helices from both sides); the active site contains the catalytic triad, Ser105(nucleophile)-His224(basic residue)-Asp/Glu187(acidic residue) and an oxyanion hole. In most cases, the active site is covered by a lid which opens in the presence of an interface to facilitate contact with the substrate [24].

Naturally, the conformational structure of the lipases is adapted to accommodate the substrate at low temperatures. Their behavior is compared with those of mesophilic and thermophilic enzymes by crystallographic studies or site-directed mutagenesis [23]. For instance is the case of *Pseudomonas immobilis* and *Pseudomonas fragi* IFO 3458 lipases which compared with their counterparts reveals that they have a very low content of arginine residues in comparison with the lisine residues, weak hydrophobic core, very few salt bridges and few aromatic-aromatic interactions. In addition, the arginine residues are distributed differently from mesophilic enzymes. Some of them are at the level of salt bridges, but most cover the surface in the idea of increasing the conformational flexibility. The high content and aggregation of glycine residues depict local mobility. Another feature is associated with the production of trehalose and exopolysaccharides, acting like

cryoprotectants for protein precipitation and denaturation. If glycine is substituted by proline, the shift in the acyl chain length enhances the thermo-stability of the enzyme [23].

Cold-active enzymes, in general, inherit heat instability, which undergoes rapid inactivation of the enzymes at moderate temperatures. For industrial applications, the needs of thermostability are crucial. The psychriphilic yeast, *Candida antarctica* expresses two lipases, namely *C. antarctica* lipase A and *C. antarctica* lipase B, with different physicochemical behavior. CAL-A is considered to be the most thermostable enzyme (>90°C), while CAL-B is smaller in size and less thermostable. The factors commonly considered to increase thermal stability are the hydrophobicity, number of hydrogen bonds, amino acid composition, amino acid distribution and interactions in the protein. Directed evolution with random mutagenesis based on error-prone PCR (epPCR) and iterative saturation mutagenesis guided by rational design are more frequently employed nowadays to combat the thermolability of these enzymes [25].

Lipase A from *Bacillus subtilis* after ep-PCR shows an increase of 15°C of the melting point and of 20°C at optimal temperature, comparing with wild-type lipase. From *P. fragi*, a variant is obtained after two rounds of evolution which displays a shift of 10 degrees in the optimal temperature. The protein engineering strategy was adapted to enhance the thermostability where the disulphide and other bonds are modified to decrease the entropy of the unfolded form of proteins or to decrease the unfolding rate of irreversibly denatured proteins. CAL-B and *Geobacillus zalihae* T1 lipase were successfully engineered by mutating five amino acid pairs to cysteine and by introducing an ion-pair in the inter-loop [23].

As stated, lipases are structurally modified to accommodate the substrate at reduced temperatures. The greatest advantage of cold-active enzymes is the consumption of a small amount of energy associated with the high flexibility of their activity under low water conditions. They are cost-advantageous, of wide variety, stable to organic solvents and specific in mild reaction conditions [23].

III. Cold-active enzyme-based esterification of silybin with fatty acids

III.1. Esterification mediated by cold-active lipases

The lipase-mediated esterification reaction has come to prominence in recent decades, due to the interest in organic esters for biotechnology and the chemical industry. The main difference between lipases and esterases consists of the occuerence of non-polar residues clustered around the active site at high accesibility values [26].

The mechanism of the lipase esterification reaction is like the one proposed for the serine-based protease-mediated reaction, involving two tetrahedral intermediates. The serine residue in the triad attacks as the nucleophile of the reaction the acid, losing a water molecule. An acyl-enzyme complex is formed. The alcohol molecule interacts through nucleophilic attack with the first tetrahedral complex to form the second intermediate. Thus, finally the enzyme releases the ester and regains its native form. The mechanism of the reaction could be analyzed in Figure 8. In nature, lipases are found to be active at oil-water interface. In vitro, they are found to be active in aqueous as well as anhydrous organic solvents. The interfacial activation was hypothesized to be due to a conformational change resulting from the adsorption of the lipases onto a hydrophobic interface, where a significant role is also held by the lid [24].

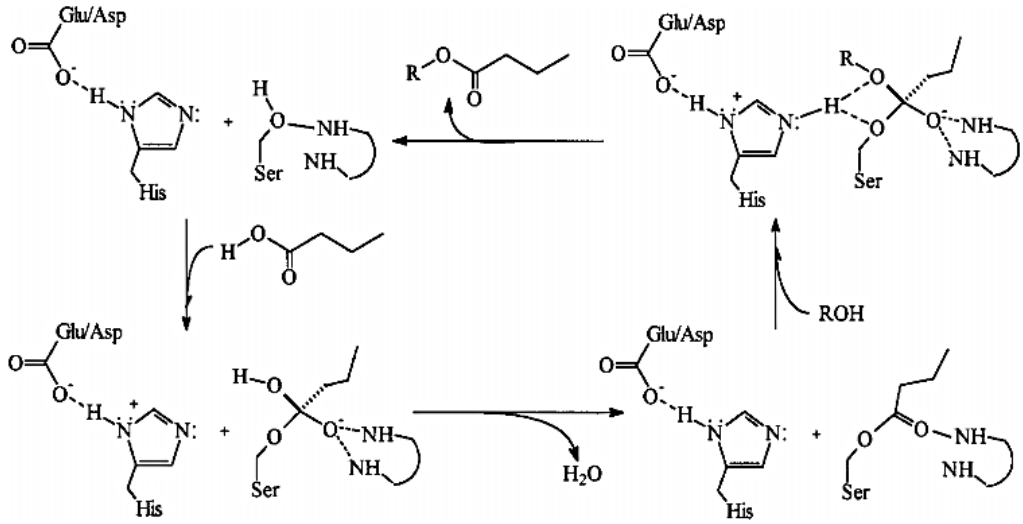

Figure 8. Mechanism of esterification by lipase catalyst.

During the esterification reaction, lipase could be deactivated due to several factors regarding temperature, exposure to interfaces, chemical denaturants, shear stress. The esterification reaction is always performed in non-aqueous solvents, in which the stability of the enzyme depends on the properties of the solvent. As Nakano et al have argued, lipase stability in organic solvent could be enhanced by random mutagenesis. Thermal deactivation of enzymes is greatly reduced by immobilization. Arroyo et al. and Moreno et al. have promulgated studies on the temperature deactivation of immobilized enzymes, having as reference lipase B from *Candida antarctica* and lipase from *Candida rugosa*. The deactivation in the case of the immobilized enzyme was much slower. Studies on deactivation of lipids in *Aspergillus oryzae* and *Candida cylindricea* under shear stress have shown that deactivation occurs due to energy consumption per unit volume and gas hold-up [24].

Saturated fatty acids are mainly involved in the production and storage of energy, being the first line of bio-components that by consuming 1 gram of lipids generates 9.3 kcal. Saturated fatty acids are also engaged in lipid transport and phospholipid and sphingolipid synthesis ensuring the

structural integrity of cellular membranes [27]. Stearic acid, the 18-carbon chain, is the most popular saturated fatty acid found in foods, but palmitic acid, the 16-carbon saturated chain, is the most prevalent in most nutrients, as well as in the body [28].

Monounsaturated fatty acids are key components due to their unsaturation, which confers a slight fluidity in the membrane lipid bilayer. Thus, they accompany monounsaturated fatty acids, displaying more structural properties [27]. Oleic acid is a major monounsaturated fatty acid, with the Cis configuration of the double bond. It is normally found in olive oil, palm oil and canola, which are promoted as monounsaturated oils. As mentioned earlier, polyunsaturated fatty acids contain two or more double bonds. Because of the cis configuration, the hydrocarbons chain aims a slightly bending, property with a special meaning in the physiological responses of fatty acids. The cis unsaturated fatty acids with their bent chains would behave in a more disorderly fashion, while the saturated and trans unsaturated fatty acids could stack together tightly exposing structural rigidity [28].

The term 'essential' for saturated and monounsaturated fatty acids are not commonly exploited, as this term is intended for polyunsaturated bio-components introduced through food intake that fulfill particular physiological functions [27].

Essential fatty acids are important constituents of cell membranes because the multitude of double bonds ensuring fluidity and affinity at the binding sites of enzymes and membrane receptors. They cannot be synthesized by the human or animal body, for which they are purchased from the diet. There are a series of essential fatty acids omega-6 derived from cis-linoleic acid and omega-3 derived from α-linolenic acid. For instance, the linoleic acid is polyunsaturated, having two double bonds, which extends the tendency to bend the chain. The common linoleic acid is an omega-6 mostly encountered in vegetable oils. There is also α-linoleic acid, a less widespread omega-3, found in flaxseed oil, canola, soy and wheat germ oil. All the omega-3 polyunsaturated fatty acids are generally considered to be essential [28]. The omega-9 series derived from oleic acid is considered not to be part of the essential fatty acids' category. However, all these series of polyunsaturated acids are metabolized similarly due to the large hydrocarbon chains, which are degraded by the same enzymes. These long-chain metabolites are of particular physiological importance in the brain, retina, liver, kidneys, gonads, adrenal glands [29].

Further it will be presented some aspects concerning the applications and implications of polyunsaturated fatty acids in the human body. The fluidity of the cell membrane is characterized by the composition of constituent lipids. Incorporation of saturated acids and cholesterol molecules increases rigidity. On the contrary, an advanced intake of unsaturated acids contributes to the formation of the fluid mosaic of the membrane, as well as to the improved response of the receptors to analogous hormones, growth factors or membrane proteins. A valuable example is insulin resistance due to the rigid membrane unable to bind insulin receptors. Thus, the therapeutic

implication of the lipid composition of the cell membranes on diabetes mellitus is outlined. Polyunsaturated fatty acids are shown to inactivate encapsulated viruses. Since neutrophils, macrophages and T cells stimulate the release of unsaturated fatty acids, it could be concluded that they are involved in the body mechanism of defense. Furthermore, their beneficial actions also sum up anti-fungal, anti-inflammatory, anti-viral and anti-bacterial responses. Studies have shown that acids have a guaranteed impact on atherosclerosis by modulating the expression of uncoupled proteins in vascular tissue [29].

III.2. Design of the biocatalyst

The immobilization technology was born in the 60s, aiming to improve the stability, reusability, activity, specificity, and manipulation of the catalyst. Conventionally, there are 4 major immobilization techniques: adsorption, covalent binding, cross-linking and entrapment, for each one knowing both the advantages and the disadvantages [30]. In Figure 9, there are outlined the immobilization possibilities, excepting the physical adhesion.

By adsorption on a solid support, a physical process itself, the enzyme retains its catalytic activity unchanged, but weak interactions between the enzyme and support can easily lead to the release of the biocatalyst. However, this method of adsorption immobilization is the most preferred [31]. A relatively small number of cold-adapted enzymes have been immobilized on solid supports such as diethyl-amino-ethyl-Sepharose or agarose-coated polyethylene-imine. For instance, cold-adapted

β-galactosidase from *Pseudoalteromonas sp.* is responsible for lactose degradation during storage of milk at low temperatures, was immobilized on DEAE-Sepharose. In this situation, the storage stability at 4°C lasted one week, but no extensive measurements have been made at higher temperatures [30].

A more modern approach refers to enzyme immobilization via covalent attachment to stimulus-responsive or smart polymer and magnetic particles. The enzyme could be easily removed from the reaction mix by applying a magnetic field for decantation or magnetically stabilized fluidized bed reactors [31]. The disadvantage in this case is that the nanoparticles oxidize in air [30]. The case of lipase immobilization on magnetic nanoparticles, initially follows an activation step with carbodiimide, the resulting suspension being sonicated and held at 4°C [32].

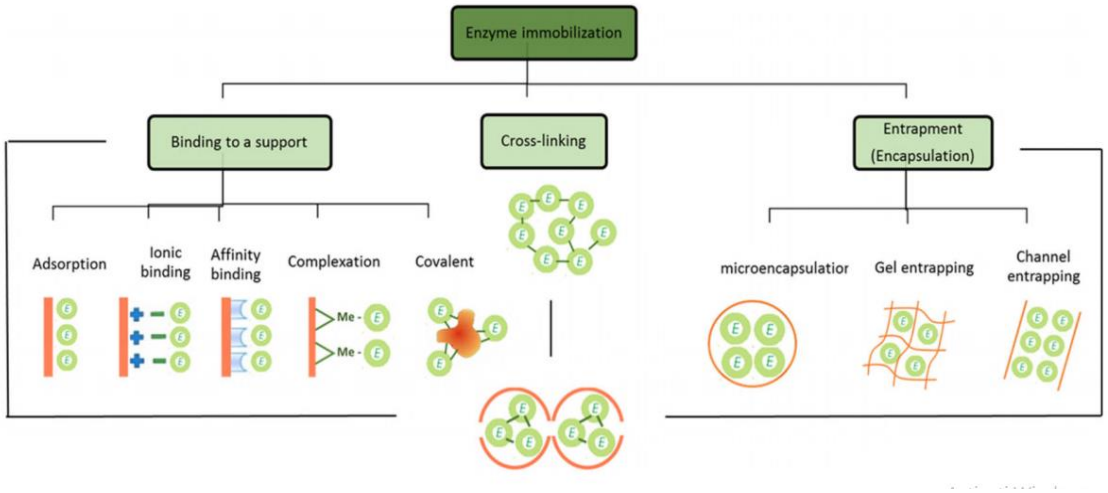

Figure 9. Enzyme immobilization techniques.

Cold-active enzymes have been covalently immobilized on several carriers, including agarose, chitosan, Sepharose, silica and graphene oxide. By covalent modifications generally the catalytic activity is diminished. Immobilization leads to the improvement of the thermal stability of the enzymes, which are markedly adapted to the temperatures considered critical, at which the enzymes begin to disorganize and destabilize. A psychrophilic pullulanase (*Exiguobacterium* sp.) starts losing its activity from 50°C, pointing no activity at 60°C. The immobilized enzymed on epoxy-functionalized silica maintains its thermal stability up to 90°C for one hour of incubation [30, 31].

Cross-linking technique aims to covalently link the enzymes together by creating aggregates. Firtly the enzymes are precipitated, then cross-linked using agents such as glutaratealdehyde or aldehyde dextran.. Enzymes could also be encapsulated into a polymeric matrix. Nonetheless, few attempts have been published on this topic. For instance, a cold-adapted cellulase from *Pseudoalteromonas* sp. was covalently immobilized in sodium alginate gel beads for the ethanol fermentation of kelp cellulose. After 7 cycles, the enzymes still show 58% activity [30, 31].

Another topic of particular importance is the use of organic solvent in enzymatic environment. This intention is industrially supported for the ease of solubilization of water-insoluble substrates, but the enzyme can be negatively denatured. Cold-adapted enzymes are more sensitive to changes in temperature, outside the optimum range, and solvent. After the first identification of organic solvent-tolerant lipase Lip9 from *Pseudomonas aeruginosa* LST-03 with increased activity in n-decane, n-octane and DMSO, many enzymes were cloned, and the enzyme tolerance to an organic solvent was improved by directed evolution. Recently, the polar organic solvents, methanol and DMSO were shown to increase the conformational flexibility of the cold-adapted and organic solvent-tolerant lipases PML (*Proteus mirabilis*) and LipS (*P. mandelii*). The armistice path for best results could treat enzymes with organic solvent if they are properly immobilized on a solid support, to maintain both their structure conformation and thermo-stability [30].

MATERIALS AND METHODS

I. Structural analysis tools

The bioinformatics tools were used for the prediction of the secondary and tertiary (modeling) structures of the putative enzymes and the analysis of their molecular weight, amino acid composition, isoelectric point, hydrophobicity, etc., based on their primary structure.

Identification of genes coding for lipases/esterases in the genome of *Psychrobacter sp*. from Scarisoara Ice Cave, and primary, secondary, and tertiary structure analyses of the putative encoded enzymes were performed as preliminary investigations. To identify the putative lipases/esterases encoding genes, screening of the genome sequence of *Psychrobacter sp.* from Scarisoara Ice Cave using BLAST program of the NCBI web site (http://www.ncbi.nlm.nih.gov/) was carried out using previously reported bacterial lipases/esterases protein sequences as a template.

I.1. Primary structure analysis

The primary structure analysis of lipases was carried out using ExPASy proteomics tools (https://www.expasy.org/) [33]. ProtParam software was used for determining the amino acid composition, atomic composition, and the total number of positively/negatively charged residues, the molecular weight (Mw), and isoelectric point (pI).

I.2. Homology and alignment of protein sequence

With the obtained putative lipases enzymes, it was performed a BLAST screening to search for primary sequence homologs. As it comes to a newly identified species from the glacier of Scarisoara Ice Cave, the need to examine the constitutive proteins properly is without a doubt.

The amino acid composition and sequence identity and similarity scores (%) between lipases' primary structure of the target bacterium and other mesophilic, hyper-thermophilic, and psychrophilic bacteria were calculated using Emboss needle online tool (http://www.ebi.ac.uk/Tools/psa/emboss_needle/) [34].

To unravel the structural adaptation characteristics alongside the primary structure and to evaluate modification in the conserved regions, primary structure alignment of various lipases sequences was carried out using the CLUSTAL OMEGA EMBL-EBI multiple sequence alignment software (http://www.ebi.ac.uk/Tools/msa/clustalo/) [35].

I.3. Secondary and tertiary structure analyses

Predicted secondary structure of lipases/esterases was obtained using the online CFSSP (Chou & Fasman Secondary Structure Prediction Server) tool (http://www.biogem.org/tool/chou-fasman/) [36].

The theoretical model of lipases 3D structure was obtained using the I-TASSER (Iterative Threading ASSEmbly Refinement) server [37]. Model visualization was performed using the Pymol software (PyMOL Molecular Graphics System, Version 1.2r3pre, Schrödinger, LLC).

II. Bacterial strain culturing

Psychrobacters usually grow well on standard complex media such as infusion agar, tryptone-yeast extract agar, or trypticase soy agar. These organisms may be found growing slowly as contaminants on plates are stored at 4°C [38].

The bacterial strain used in this study belongs to *Psychrobacter SC65A.3* isolated from Scarisoara Ice Cave (Romania), which was extracted and completely analyzed in terms of taxonomic affiliation and microbiological characteristics by V. Paun (manuscript in preparation).

The bacterial strain cultivation was properly performed at 15°C in Trypticase soy (Scharlau Microbiology) (Table 3) and Reasoner's 2 (Melford Biolaboratories Ltd.) (Table 4) culture media (broth and agar).

Table 3. Composition of the Trypticase soy culture medium.

	Composition	**Chemical ole**
Tryptic soy broth	Casein peptone 17g/l	Assortment of peptides assuring the amino acids and nitrogenous substances as a nutritious content
	Soy peptone 3g/l	Nutritious content of amino acids for bacterial growing
	Sodium chloride 5g/l	Maintain the osmotic equilibrium
	Dipotassium phosphate 2.5 g/l	Maintain pH
	Dextrose 2.5g/l	Source of energy through carbohydrates cycle

The pH of the medium was adjusted to 7.3 at 25°C and further sterilized in the autoclave at 121°C for 15 minutes. For the corresponding solid medium, a suitable amount of agar was added to accomplish a final concentration of 15 g/L.

Table 4. Composition of Resoner's culture medium.

	Composition	Chemical role
Reasoner's	Proteose peptone 0.5g/l	Assortment of peptides assuring the amino acids and nitrogenous substances as a nutritious content
	Magnesium sulphate 0.1g/l	
	Sodium pyruvate 0.3g/l	
	Casein acid hydrolysate 0.5 g/l	Amino acid source
	Dipotassium phosphate 0.3g/l	Maintain pH
	Yeast starch 0.5g/l	
	Soble starch 0.5g/l	Glucose polymer as an energy source
	Glucose 0.5g/l	Carbon energy source

For Reasoner medium preparation, 3.2 g of the standard mixture will be dissolved into 1 liter of distilled water and sterilized in the autoclave for 15 minutes and the agar medium containing 1.5% agar as a final concentration.

III. Biochemical methods

III.1. Plate screening assays

For measuring the extracellular lipolytic activity of the *Psychrobacter SC65A.3* strain, the assays implied using different substrates such as: tributyrin 1%, Tween 80, Rhodamine B and, calcium chloride (Sigma Aldrich, Germany), and olive and sun-flower vegetal oils for commercial use.

The ability of *Psychrobacter* sp. strain to synthesize lipases was evidenced by cultivation on TSA and R2A culture media supplemented with 1% olive oil and 0.001% rhodamine B. Rhodamine solution was previously sterilized by filtration through a Millipore membrane of 0.22 µm. Volumes of 150 µL of the bacterial culture in the logarithmic growth phase were plated on Petri dishes containing solid media and incubated at 15°C for 96h. Lipase activity was detected by irradiating the Petri dishes with ultraviolet light at a wavelength of 350 nm leading to the appearance of a red-orange fluorescent halo, around the growth area of the bacterial strain [39]. The tests were performed in duplicate. The oils were added to the culture media after the media sterilization [40].

The culture media containing 1% tributyrin was sterilized for 20 minutes at 121°C and distributed in Petri dishes. The inoculation was performed as a spot on the surface of the culture media. Petri dishes were incubated for 7 days at 15°C, and the positive reaction was indicated by the appearance of a transparent halo around the bacterial culture. Similar manipulation applied for 1% Tween 80 assay, where the culture medium supplimentary contains 0.01% $CaCl_2 \cdot 2H_2O$. The lipase

reaction was positive as off-white calcium oleate microcrystals were formed as a response to the biocatalytic hydrolysis around the reaction zone.

Direct quantitation of lipase activity is difficult, presumably because of the low amounts of lipase molecules released by a single colony. Quantification could be done, however, by filling culture supernatants into holes punched into the agar. The logarithm of lipase activity is linearly related to the zone diameter [39].

III.2. Extraction of the protein content

Psychrobacter cells cultured in Reasoner's medium were centrifuged at 4800 rpm for 20 minutes at 4°C to separate the culture supernatant containing extracellular proteins, including the two previously characterized lipases, from the cell debris. The culture medium was supplemented with 1% olive oil to increase extracellular lipase production as the literature specifies that the preferred carbon source for extracellular lipolytic protein production comes from oils and not from sugars/carbohydrates as usually expected for general microorganism culture [41]. The purification was performed by extraction with organic solvent. It was used 80% acetone to precipitate extracellular protein content from culture media using a 2/1 volumetric ratio. Adding drop by drop the solvent solution, the protein precipitate was obtained on ice and left overnight to completely settle [42]. The precipitate was then centrifuged at 10 000 rpm for 10 minutes and collected in Eppendorf tubes left unlocked to assure acetone evaporation. In this way, the newly formed protein extract was resuspended in 100 mM TRIS-HCl pH 7.5.

III.3. Determination of enzyme concentration

Aliquots of known concentrations, prepared from bovine serum albumin (Sigma Aldrich-Merck) in distilled water were used to achieve the standard curve within 0.1-0.9 mg/mL linearity range at 280 nm. The precipitate concentration was evaluated by interpolation within the standard curve.

III.4. Determination of enzyme activity

The following materials were used for the enzymatic activity: p-nitrophenyl butyrate/palmitate, Triton100, TRIS-HCl buffer, sodium carbonate, all being purchased from Sigma Aldrich-Merck, except for Triton100 which was kindly offered by Institute of Chemistry-Physics, Bucharest. The standard method for determining lipase activity involves changing to yellow the color of the newly formed phenol product and reading its absorbance at 347 and 410 nm, respectively as

agreed in the protocol. UV-VIS analysis was performed on a standard spectrophotometer (Specord 250, Analytik Jena), using 1 cm path length cuvettes.

Stock solution of 1 M TRIS-HCl (tris(hydroxymethyl)aminomethane hydrochloride) buffer was prepared by dissolving 6 g of TRIS base in 50 mL distilled water, while adjusting the pH value to 7 with concentrated hydrochloric acid. Proper dilution was then achieved in distilled water for 100 mM TRIS-HCl buffer. All the reagents involved in buffer preparation were supplied by Sigma Aldrich-Merck.

The reaction mixture was set as follows 0.25 mL protein extract, 0.65 mL 0.1 M TRIS-HCL pH 7, 0.1 mL 0.025 M substrate (p-nitrophenyl butyrate and p-nitrophenyl palmitate) dissolved in ethanol, and incubated for 30 minute at 25°C and 37°C. A blocking solution of 0.1 M Na_2CO_3 was used to stop the reaction after 30 minutes. Meanwhile, the reaction mixtures were centrifuge at 8000 rpm for 2 minutes in order to allow the immobilized extract to settle. The absorbance values were read at 347 nm, while plotted against the calibration curve realized on p-nitrophenol substrate of known concentrations dilluted in ethanol solvent.

IV. Chemical methods

IV.1. Enzyme immobilization

Two methods of immobilization were approached. Covalent immobilization via glutaraldehyde (Sigma Aldrich-Merck) linker was performed on amino-C_2-methacrylate type resin, using two buffers to mediate the reaction: PBS (phosphate buffered saline) and MES (2-(N-morpholino) ethanesulfonic acid) buffer. The support, kindly offered by the Purolite Life Sciences Company, is in the form of spherical beads (150–300 μm of diameter) originally functionalized with -NH_2 groups using methacrylate crosslinker polymer. 0.1 g amino–C_2–methacrylate support reacted with 0.1% glutaraldehyde and 100 μL protein extract in MES (pH 4.7) or PBS (pH 7.4) buffers for 2 hours under stirring [43]. The reaction mixture was centrifuged at 2000rpm for 10 minutes and the supernatant containing the unattached protein extract was separated from the resin beads with the immobilized proteins. Washing step and resuspension of resin beads was done in PBS pH 7.4 buffer 3 times.

MES buffer (pH = 4.7) used for modification of resin surface was prepared by dissolving MES solid in distilled water to a final concentration of 10 mM, followed by the addition of NaOH for adjusting the pH value of the solution to 4.7. Ten milli molars of PBS solution (pH = 7.4) was used as aqueous buffer solution. Its composition consisted of: 8 g NaCl, 0.2 g KCl, 1.43 g Na_2HPO_4 ×

$2H_2O$ and 0.34 g KH_2PO_4 in 1 L distilled water. All of the reagents used for the preparation of MES and PBS buffers were purchased from Merck and Sigma-Aldrich, respectively.

Covalent immobilization on the functionalized surface of magnetite particles was experimented on Chemicell beads. The carbodiimide method involved the use of EDC, PBS / MES wash buffers and blocking and storage solution prepared in PBS with 0.1% bovine serum albumin and 0.05% sodium azide, all purchased from Sigma Aldrich-Merck.

1 mL of comercial suspension of Si-MAG-amine, Si-MAG-carboxyl and Fmp-carboxyl magnetic particles was washed and resuspended in MES buffer pH 6, proceeding further the same protocol of immobilization on both supports through carbodiimide method. The magnetic beads were gathered with a magnetic separator and foremost mixed with 0.25 M EDC in MES buffer. The immobilization reaction happened for 2 hours at room temperature and gently shaking after the addition of 200 µL of 6.6 mg/mL protein extract

Prior to the immobilization on Si-MAG-Hydrazine particles, 500 µL protein extract was incubated with 5mg $NaIO_4$ in the dark at room temperature for 30 minutes. Then, the magnetic beads were placed to react with 0.25mL of newly oxidized protein extract for 6 hours at room temperature (Figure 6.). The blocking and storage solution in all assays was PBS buffer pH 7 containing 0.1% BSA and 0.05% NaN_3. Gentle oxidation of the glycosidic groups within the protein extract was accomplished with sodium periodate (Sigma Aldrich-Merck).

IV.2. Characterization of biocatalyst

FTIR spectra of bio-composites and simple/functionalized supports were recorded using Vertex 70 (Bruker, Ettlingen, Germany) spectrophotometer equipped with the Diffuse Reflectance Infrared Fourier Trnasform cell. Sixty four scans were collected with a resolution of 4 cm^{-1} in the wavenumber range of 400–4000 cm^{-1}.

IV.3. Biocatalytic system

1 mg of silybin was weighted and dissolved in 1 mL THF solvent, while adding 10 µL of fatty acid/ester. After throughly mixing the substrates, 100 µL of protein specimens, either free or immobilized, were added to reaction, while incubating at 25°C for 24 h at 1000 rpm. The reaction mixtures were then centrifuged for 15 minutes at 1500 rpm, allowing the enzyme extract or the immobilized to settle, while collecting the supernatant. Reaction mixtures were passed through 0.22 µm milipore filters into HPLC vials and left in the oven at 70°C for complete evaporation of the solvent. Final preparative step resumes at total solvation of the unreacted substrates and transformed products into mobile phase of the chromatographic analysis.

The catalytic performances of the above-mentioned system were analyzed by the HPLC-DAD method using a 1260 Infinity HPLC modular system from Agilent Technologies equipped with a Poroshell 120 EC-C18 column and a diode array-type detector (DAD). The experimental parameters of the analysis were as follows: acetonitrile and water (41/59, v/v) mixture as mobile phase, 1 mL/min flow rate and 25 μL injection volume, while the chromatogram was recorded for 30 minutes.

RESULTS AND DISCUSSIONS

I. Structural analysis

I.1. Primary structure analysis

Sequence homology

A BLAST screening of the genome of *Psychrobacter SC65A.3* isolated from the perennial ice block of Scarisoare Ice Cave led to the identification of multiple genes encoding for lipases and esterases. Among these, the deduced amino acid sequence of the putative Lipase 2_65A.3 and Lipase 3_65A.3 (Table 5) was selected for evaluating the structural elements related to a cold-adaptation mechanism that necessities to be adequately elucidated.

Table 5. Protein sequences of the two lipases selected from *Psychrobacter SC65A.3* proteome.

	Protein sequence
Lipase 2_65A.3	MSNSTVLSVNTLLNKAVKTLNLMSFGQDKNPKSTDINLSDEIIDIEESALQDSREDKGLSIKEKILEHHLMTNYQP HLLHYAIKSFGCLPTPILESLIKCLDGPTSKQYLHVDAHLRLILAVNSKLKTPLQLIEMSELRKRFATDAVAMQAP KVWQQASDNLLSNLKQFHKK**GDSA**ISWQDRTITNADDGDMTIRCYQNETSDNGFGFKKEQTSNPDETVLLFF**H GGGF**CIGDLNTHHEFCHAICEQTGWPVISVDYRLAPEHPAPAAVRDCISAYAWLAEHCEEFGALPSRIVLA**GDS A**GGGLSTLMAQQIITPNKEAWLDLGDEGQKTFDILQGLPHPMAQMPLYPVTDIETDYPSWELYGEGLLLDHAD VAIFDAACLENSPLPRQHILTSPMLGDNRQVCPSYVVAAELDVLRDEAFAYANQLKSFGIAVQTHTVLGA**PHG**F IHFMSVHQRLGQETQHIITGFANFVREIIKTRALLSA
Lipase 3_65A.3	MLLKRLGLATLLSFSVVGCTTAPNTLAINTTQKIIQYERSKSDLTTQSFTLSSGDKIVYAENGNVAGEPLLLI**HGF GG**NKDNFTRIARQLENYNLIIPDLLGFGDSSKPMAADYRSEAQATRLHELLQAKGLASNIHVG**GNSMG**GAISV AYAAKYPKEVKSLWLIDSAGFWSVGVPKSLESATLENNPLLVDKKEDFYAMYDFVMSKPPYIPKSVKAVFAQE RIANKAVESKILAQIVEDNVEQRAKVIAEYNIPTLVVWGEEDKVIKPETVTLIKEIIPQSQVITMPKIGHVPMIEAV KDTANDYKAFREGLKN

Pair alignment of deduced amino acid sequences using Emboss needle software provides the identity and similarity scores of the two lipases from *Psychrobacter SC65A.3* with homologs from psychrophilic *Psychrobacter* sp. *G*, *Glaciibacter superstes*, and *Moritella sp. PE36*, mesophiles *Escherichia coli* and, *Pseudomonas aeruginosa* and, hyperthermophile *Strenothopomonas maltophilia* (Table 6). An alternating debate over their structure, composition, and the tendency will be further taken. Reference codes for every bacterial strain above-mentioned will be found in the ANNEX 1.

Both Lipase 2_SC65A.3 and Lipase 3_SC65A.3 showed the highest identity score (99%) with one psychrophilic species, while much more reduced (28%) with the other two psychrophilic strains. Interestingly, the identity and similarity scores of the two SIC originating lipases were somewhat higher with the homologs from both mesophilic bacteria (29-33% / 43-48% and 26-37% / 43-58%, respectively) and hyperthermophile (30% / 41% and 35 / 57%, respectively), suggesting a more complex thermal-adaptation mechanism related to structural composition.

Table 6. Identity and similarity scores for the two lipases of *Psychrobacter sp. SC65A.3* with homologous enzymes from psychrophilic, mesophilic, and thermophilic microorganisms.

	Lipase homologs	Lipase 2_65A.3		Lipase 3_65A.3	
		Identity (%)	Similarity (%)	Identity (%)	Similarity (%)
Psychrophiles	*Psychrobacter sp. G*	98.96	99.37	99.68	99.68
	Glaciibacter superstes	28.88	43.10	27.75	43.54
	Moritella sp. PE36	28.24	43.92	27.67	42.76
Mesophiles	*Pseudomonas aeruginosa*	32.78	48.96	36.92	58.06
	Escherichia coli	29.08	43.32	26.33	43.41
Hyperthermophile	*Stenotrophomonas maltoflia*	30.43	41.47	35.11	57.44

The highest identity score (98.96%) of Lipase 2_65A.3 was achieved with the α/β-hydrolase from *Psychrobacter sp.* G (WP_020444543.1, identified in the literature as Lip-1452 [44]), along with a considerable homology of 98.55% with *Psychrobacter cryohalolentis K5* [45] (ABE76235.1) (not shown in the table). While for Lipase 3_65A.3, **t**he highest homology (99.68%) was achieved with the α/β-hydrolase from Psychrobacter sp. G (WP_020442424.1, identified in literature as Lip-948 [44]). By comparison with *Psychrobacter cryohalolentis K5* proteome [45], it also reveals a high homology of 98.10% (ABE73807.1) (not shown in the table).

Thus, a clear identity between lipases from *Psychrobacter sp.* of SIC and *Psychrobacter sp. G* should be firstly stated, as the protein enzymes are established to be charged with the same functionality in the cell.

Interestingly, the homology scores with the two cold-active lipases from *Glaciibacter* and *Moritella* sp. were very different, showing the lowest identity and similarity and suggesting that enzymes could have evolved a series of analogous cold modifications. Still, the habitat, nutrient supplies, or other physicochemical parameters are the drivers of crucial structural thermal adaptation. Even with the mesophilic *P. aeruginosa*, the scores are particularly low, but still the highest by comparison with the overall homologous values, as the explanation sustaining that the species belong to the same Pseudomonadacee family.

Protein size and pI

Analysis of protein sequences of the two lipases using ProtParam software indicated that Lipase 2_65A.3 encounters a total number of 483 amino acids, a molecular weight of 53626.97 Da and the theoretical pI of 5.33 (Table 7/a), while Lipase 3_65A.3 comprises a total number of 315 amino acids corresponding to a molecular weight of 34606.86 Da and with a theoretical pI of 6.93 (Table 7/b). In comparison, the total number of negatively charged residues of Lipase 3_65A is 60, while the total number of positively charged residues is 38, and for Lipase 2_65A3 an equal number (35) of both positively and negatively charged residues, indicating a distinct overall charge of the two lipases.

Table 3. Dimension, molecular weight and theoretical isoelectric point (pI) of homologous lipases from psychrophilic, mesophilic and, hyperthermophilic strains.

a) Homologous lipases	**No. of amino acids**	**Molecular weight (Da)**	**Theoretical pI**
Psychrobacter sp. SC65A.3 Lipase 2_65A.3	483	53626.97	5.33
Psychrobacter sp. G	483	53527.84	5.33
Glaciibacter superstes	321	33908.18	4.75
Moritella sp. PE36	305	34088.98	6.13
Pseudomonas aeruginosa	321	34743.32	4.72
Escherichia coli	322	35255.95	5.19
Stenotrophomonas maltoflia	308	32737.20	4.78
b) Homologous lipases	**No. of amino acids**	**Molecular weight (Da)**	**Theoretical pI**
Psychrobacter sp. SC65A.3 Lipase 3_65A.3	315	34606.86	6.93
Psychrobacter sp. G	315	34650.96	7.72
Glaciibacter superstes	209	21844.94	4.74
Moritella sp. PE36	334	36512.78	4.96
Pseudomonas aeruginosa	315	34820.18	6.09
Escherichia coli	301	34348.64	8.54
Stenotrophomonas maltoflia	311	34898.25	6.00

The size of the psychrophilic enzymes corresponds to a larger protein chain as compared to that of the mesophilic (*E. coli or P. aeruginosa*) and hyperthermophilic (*Stenotrophomonas maltoflia*) homologous enzymes, with the general assumption of shortening the enzyme sequence at increasing environmental temperatures. The largest protein chains were found for the cold-adapted enzymes, while with the tendency of increasing heat, lower chains are expected for the hyperthermophilic species (Table 7).

On the values of the theoretical pI, it could not be assumed a particular tendency according to data from the tables. Generally speaking, a more acidic pI suggests structural mechanisms for low-temperature adaptation of the surface of the enzyme in psychrophilic bacteria. Lipase 2_65A.3, along with its cold-active homologs, are represented by an acid pI, but no specific changes are observed for the other enzymes [46]. While for Lipase 3_65A.3 and its cold-active series, a slight difference might be agreed to the mesophilic counterparts.

It could be considered that for a protein with the same functionality, the molecular weight would be oriented around equal value. A particularly exciting aspect stays at the level of the molecular weight of Lipase 2_65A.3 as being a doubled value comparing to the other enzymes. The first supposition is that this enzyme might be a homo-dimer and later on, the study will be sustained.

Amino acid composition

The values for the amino acid composition on each participant are listed in tables found in the ANNEX 2 at the end of the thesis.

In the first instance, Lipase 2_65A.3 from *Psychrobacter SC65A.3* is represented by a lowered amount of bulky aromatic residues as many flexible nonpolar amino acids are responsible for the structural flexibility of the enzyme in cold environments (Phe + Tyr + Trp = 7.4 % < Gly + Ala + Val + Leu + Ile + Met + Pro = 44.2%) [46].

Cysteine units cause the formation of interchain disulfide bonds intended for lower protein flexibility providing higher stability [47]. Interestingly, cysteines are present in the structure of the cold-active enzyme of *Psychrobacter* SC65A.3. In comparison with its counterparts, the considerable high value of His and Met residues are established for structure stability at low temperatures; a slight decrease of Glu content along with Asp proved the reduction of ionic interactions. Decreasing the number of Gln residues along with a higher number of Lys residues and lower Pro content stand for the overall thermal lability of the enzyme, which was also proved by the computed value of the instability index: 44.26; this classifies the protein as unstable.

On behalf of Lipase 3_65A.3 from *Psychrobacter* sp. of SIC, flexible nonpolar amino acids are widely spread along the protein chain, comparing with the aromatic ones (Phe + Tyr + Trp = 7.7 % < Gly + Ala + Val + Leu + Ile + Met + Pro = 47.2%). An alternating discussion over amino acid composition in all homologous enzymes reveals that the Cys content is comparable, while that of Met is higher in Lipase 3_65A.3, and His and Pro contents are reduced. The number of Glu residues is higher in comparison with the cold-active homologs but slightly small by evaluation with mesophilic *Pseudomonas aeruginosa*. This concludes a reduced number of ionic interactions over the whole protein. Considering the instability value for this lipase (35.91), it could be easily assumed that it is more stable than Lipase 2_65A.3.

Salt bridges

The (Arg / Arg + Lys) reports were calculated for each homolog (Table 8) to evaluate the salt bridges' impact on protein structure [48].

A typical cold-adaptation mechanism that supposes high-value reports in analogy with a reduced formation of salt bridges is observed just in the case of homologous enzymes from *Glaciibacter superstes* [47]. It was expected increased flexibility for the cold-active proteins [48], but for lipases of *Psychrobacter* sp. *SC65A.3* and *Moritella* sp., a rigid packing of the chains, stabilized by a high number of salt bridges, probably prevents cold protein denaturation.

Unexpectedly large values for mesophilic and hyperthermophilic enzymes revealed that the small number of salt bridges is not the main responsible for the lipase stability.

Table 8. Ratio of Arg and Lys residues to evaluate the presence of salt bridges.

Homologs	**Arg / (Arg + Lys)**	**Homologs**	**Arg / (Arg + Lys)**
Psychrobacter SC65A.3 Lipase 2	0.39	***Psychrobacter SC65A.3* Lipase 3**	0.26
Glaciibacter superstes	0.82	**Glaciibacter superstes**	0.86
Moritella sp. PE36	0.47	**Moritella sp. PE36**	0.43
Escherichia coli	0.89	**Escherichia coli**	0.81
Pseudomonas aeruginosa	0.88	**Pseudomonas aeruginosa**	0.72
Stenotrophomonas maltophilia	1	**Stenotrophomonas maltophilia**	0.84

I.2. Conservation and alignment of cold-active lipase sequences

Pair alignment of the cold-active lipases *SC65A.3* with those of the *Psychrobacter* sp. *G* homologs (Figure 10), indicated high conservation of their primary sequences with just one replacement of conserved and one partially conserved residues.

Lipase 2_65A.3

The intensive study of the literature was based on the high homology between Lipase 2_65A.3 from *Psychrobacter* sp. *SC65A.3* and Lip-1452 from *Psychrobacter* sp. *G* (Figure 11) [44], through CLUSTAL OMEGA pair alignment, to determine the conserved characteristics of the Lip-1452 as being overexpressed in Lipase 2_65A.3. Based on the conserved catalytic triad and overall identity of the amino acid sequences, Lip-1452 was identified as a member of the hormone-sensitive lipase (HSL) group, namely family IV of the bacterial lipases. Lip-1452 had the catalytic triad (Ser-His-Asp) and contained an oxyanion hole to stabilize the tetrahedral intermediate.

The two conserved motifs, HGGGF and GDSAG of lipases, could be identified in the amino acid sequences of Lip-1452 and Lipase 2_65A.3. The pentapeptide GDSAG contained Gly297 and Ser299 of the SIC enzymes. Perhaps Asp414 and His444 were the second and third members of the triad, respectively. The conserved Asp414 in a consensus sequence LDXL and the His constituting the triad was preceded by a Pro and followed by a Gly. All these characters indicated that Lip-1452 was a member of the HSL motif of bacterial lipases. These structural items are found in Lipase 2_65A.3 indicating that this enzyme belongs to Family IV of lipases.

Lipase 3_65A.3

Considerable sequence homology was also found between Lipase 3_65A.3 from *Psychrobacter* sp. from Scarisoara Ice Cave and Lip-948 from *Psychrobacter* sp. G (Figure 12) [44].

In Lip-948, the two conserved motifs, HGFGG and GNSMG, were identified. Lip-948 belongs to family V, based on sequence alignment, especially for the two conserved regions HGFGG and GNSMG. Moreover, Ser142, Asp264, and His292 composed the catalytic triad. It probably contained a signal peptide (Met1-Ala27), which indicated that Lip-948 might be a secreted protein. Lipase enzyme from *Psychrobacter* sp. *SC65A.3* fulfills all the structural requests above by overexpressing the same conserved motifs of Lip-948. It could be concluded that Lipase 3_65A.3 belongs to the Family V of lipases.

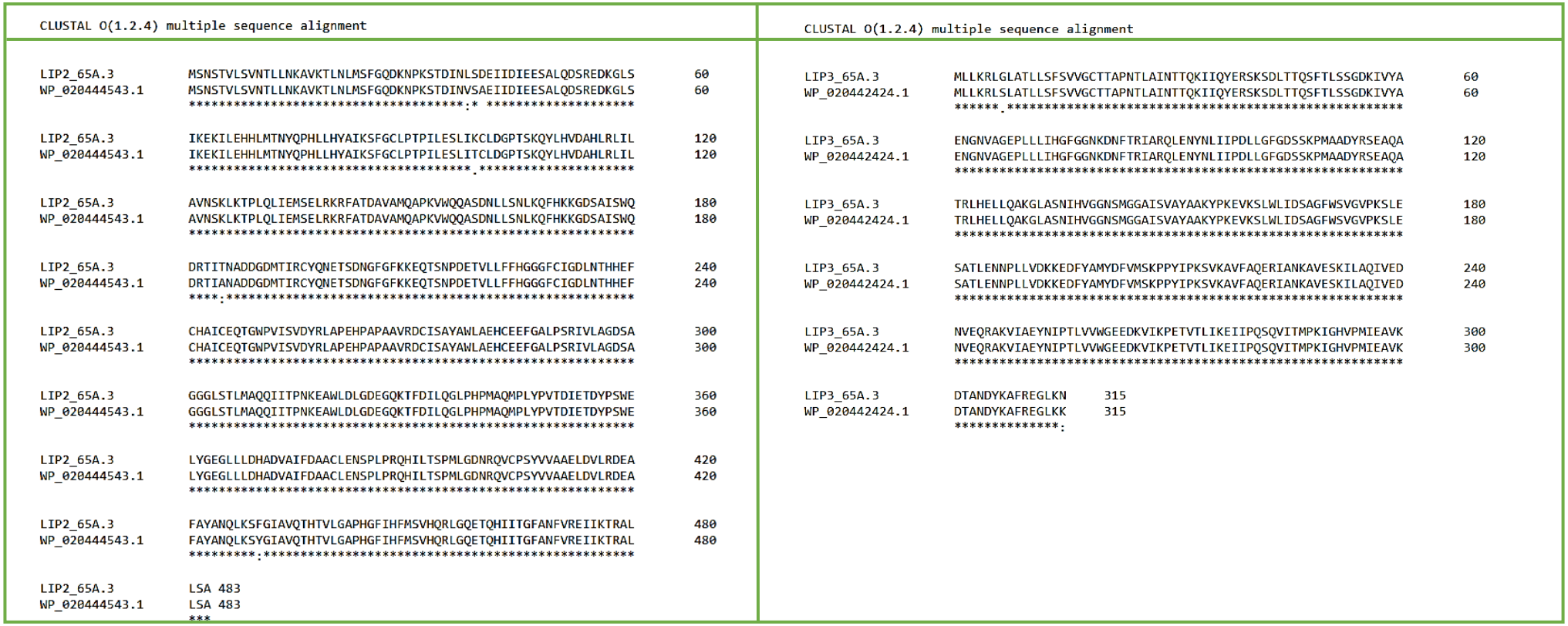

Figure 10. CLUSTAL multiple sequence alignment of Lipase 2_65A.3 and Lipase 3_65A.3 from *Psychrobacter* sp. of SIC and Lip-1452 and Lip-948, respectively, from *Psychrobacter G*. Legend:(*) identical residues; (:) conserved residues; (.) partially conserved residues.

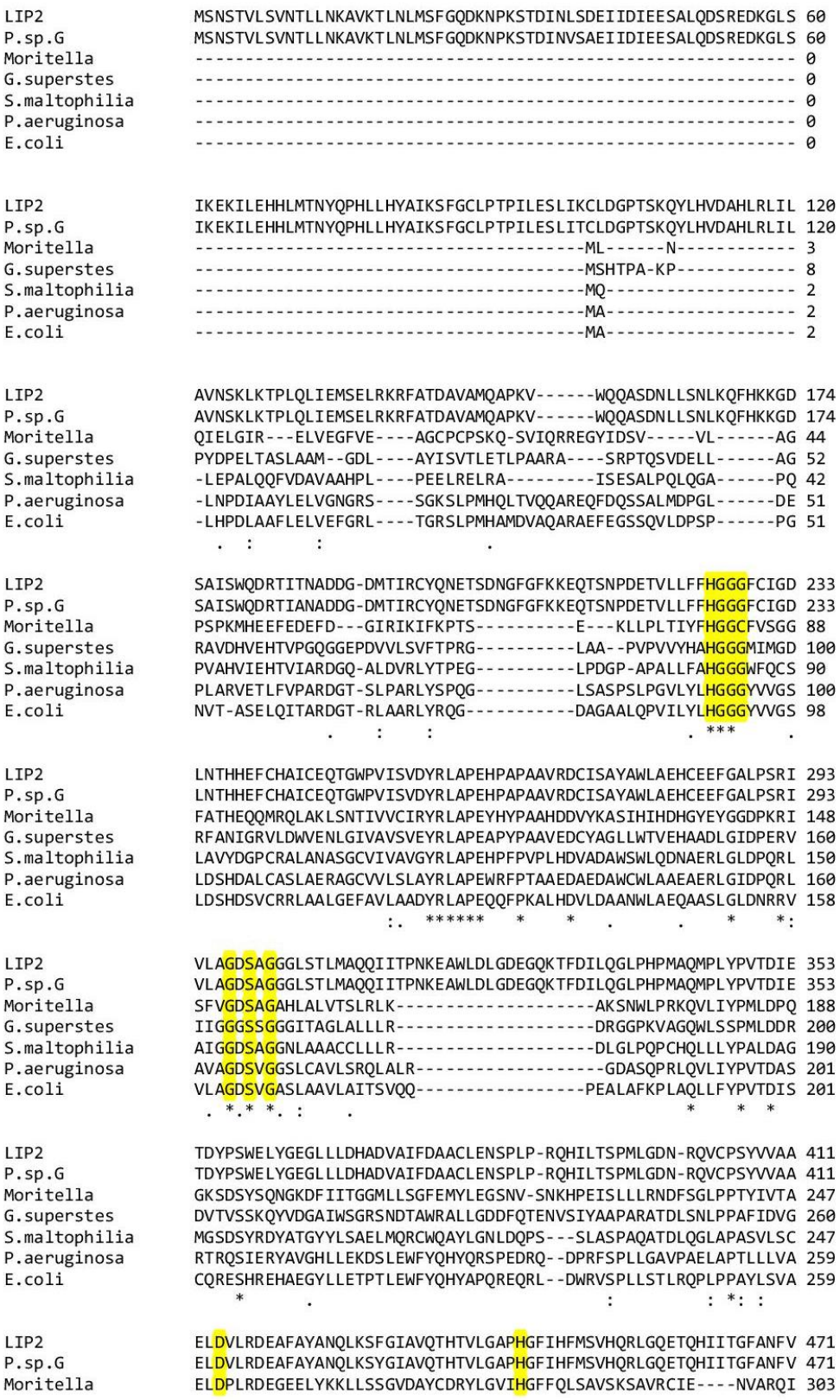

Figure 11. Amino acid sequence alignment of Lipase 2_65A.3 with the homologous enzymes by framing the common catalytic pocket and conserved motifs.

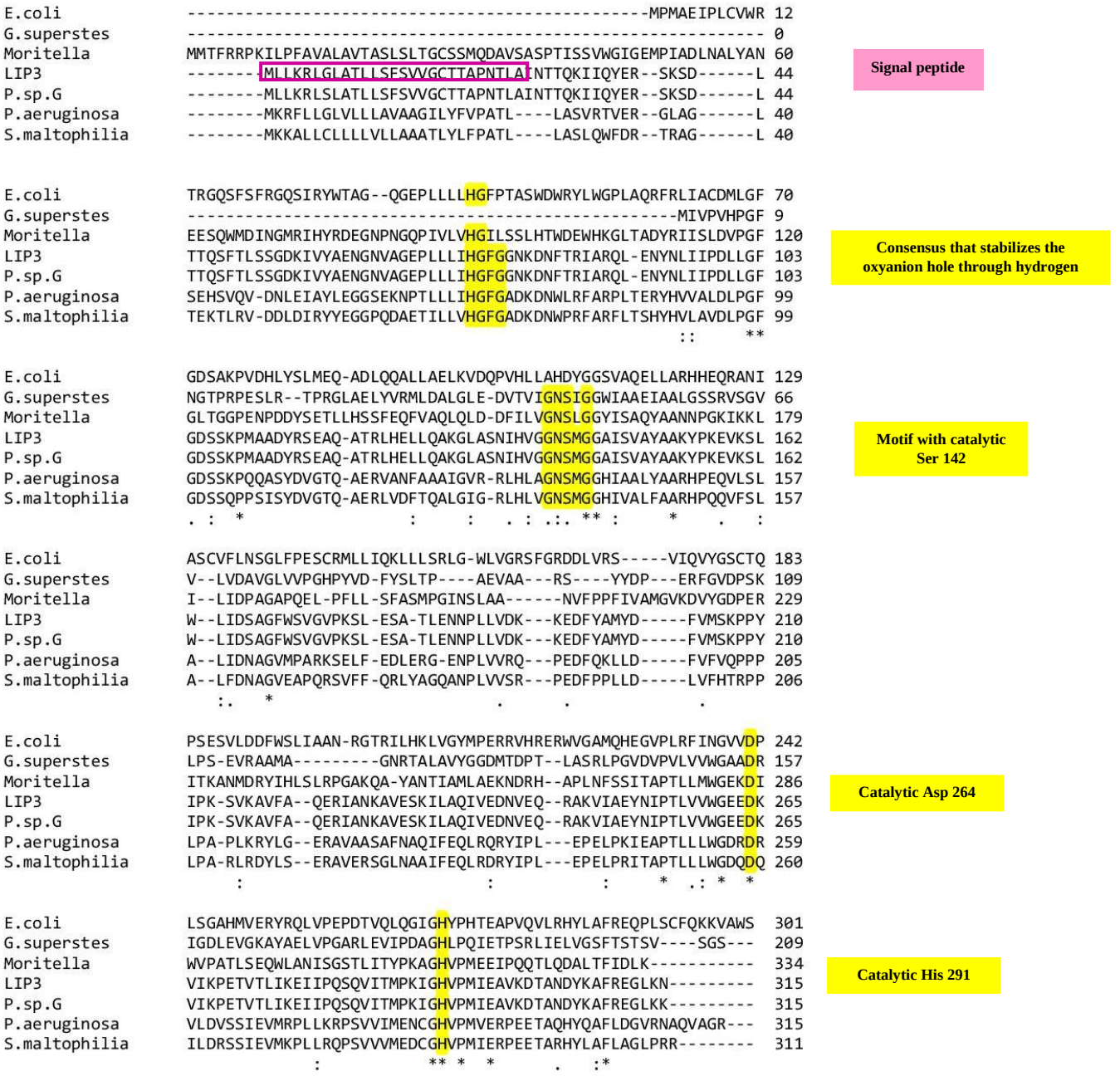

Figure 12. Amino acid sequence alignment of Lipase 3_65A.3 with the homologous enzymes by framing the common catalytic pocket and conserved motifs.

I.3. Secondary structure analysis

Secondary structure alignment of psychrophilic, mesophilic and hyperthermophilic homologous chains (Table 9) indicated a variable distribution of helices and turns, with a relatively high content of random coils in the amino acid sequence of the psychrophilic enzymes. The temperature-dependent secondary structure appeared to be related to a decreased content of turns for lipases 2_65A.3 and 3_65A.3 from *Psychrobacter* SC65A.3 compared to the *P. aeruginosa* homolog.

Table 9. Analysis of the secondary structure composition.

Homologous proteins	Secondary structure composition (%)			
	Helix	**Sheet**	**Coil**	**Turn**
***Psychrobacter sp.* SIC Lipase 2**	50.1	31.9	11.4	6.6
Glaciibacter superstes	51.4	28.7	13.4	6.5
***Moritella sp.* PE36**	40	37.4	15.7	6.8
P. aeruginosa	46.7	31.8	14.3	7.2
Escherichia coli	51.2	35.4	7.8	5.6
Stenotrophomonas maltophilia	47.1	34.4	12	6.5
Homologous proteins	**Secondary structure composition (%)**			
	Helix	**Sheet**	**Coil**	**Turn**
***Psychrobacter sp.* SIC Lipase 3**	57.8	25.4	10.1	6.7
Glaciibacter superstes	34.5	37.3	19.1	9.1
***Moritella sp.* PE36**	39.5	45.2	10.2	5.1
P. aeruginosa	64.8	21	7.9	6.3
Escherichia coli	39.5	37.2	17.3	6
Stenotrophomonas maltophilia	49.8	28.6	14.5	7.1

Interestingly, the coil content of Lipases 2_65A.3 is significantly higher than that in the mesophilic *E. coli*, while for Lipase 3_65A.3 this particular assumption could be made with the *P.aeruginosa* representative, suggesting that their position in the amino acid sequence could play a critical role in the protein folding and flexibility to adapt the catalytic process to extremely low

temperatures. A lower sheet content was also observed in lipases from *Psychrobacter* sp., confirming the reduced ionic interactions [47] in comparison with the mesophilic and hyper thermophilic enzymes, as described above. No major differences were observed in the case of helix structures that are almost equally represented.

Meanwhile, the cold-active lipases preserved independent behaviors. Lipases from *Psychrobacter* SC65A.3 showed high secondary structure conservation with the mesophilic enzyme.

I.4. Tertiary structure analysis

The 3D model of Lipase 2_65A.3 from *Psychrobacter* sp. SIC was calculated using metagenome-derived esterase Est8 as a template (PDB: 4YPV.A). The sequence identity is low (30%) because of the homo-dimer structure prediction.

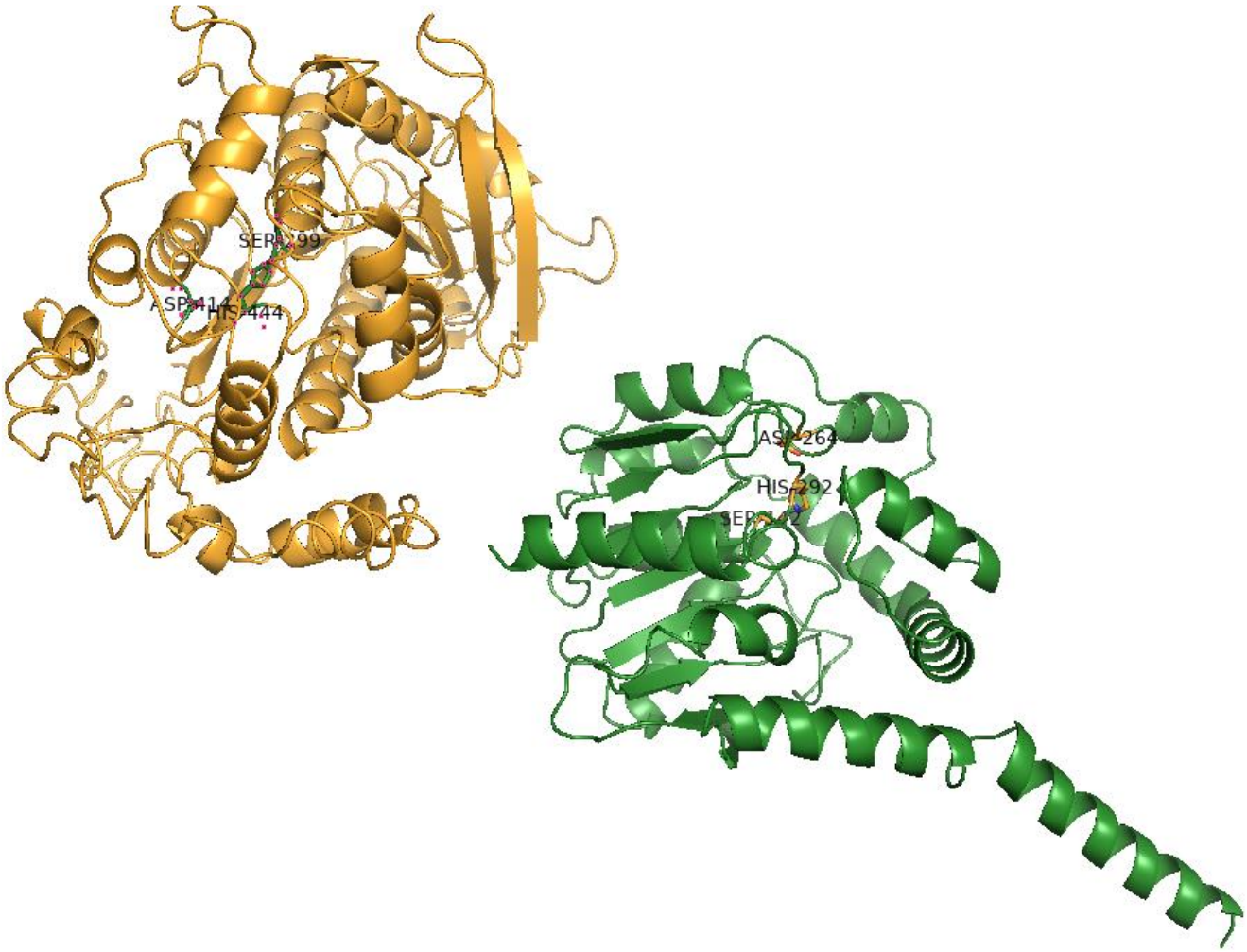

Figure 13. Tertiary structure of Lipase 2_65A.3 (yellow) and Lipase 3_65A.3 (green) predicted by 3D modeling.

In the case of Lipase 3_65A.3 3D modeling, the closest tertiary structure was superimposed with that of a cold-active esterase from *Psychrobacter cryohalolentis* K5T (PDB: 4NS4.A) used as the template. The sequence identity emerged with 98.1% coverage and the oligo-state prediction reveals a monomer.

II. Lipolytic activity. Plate screening assays.

II. 1. Lipolytic activity on tributyrin

The inoculation was performed as a spot on the surface of the culture media. Petri dishes were incubated for 7 days at 15°C, and the positive reaction was indicated by the appearance of a transparent halo around the bacterial culture. The diameter of the hydrolysis zone represents the intensity of the enzymatic activity so that the larger hydrolysis zones, the more intense activity [~~16~~ 40].

No activity was recorded in the presence of tributyrin (Figure 14). Although the bacterial strain used the culture media to grow, being more visible in the case of TSA media.

Figure 14. Petri dishes with 1% tributyrin assay.

II. 2. Lipolytic activity on Tween 80

The lipase reaction was positive as off-white calcium crystals were formed and visible on the hydrolysis zones (Figure 15). After seven days of incubation at 15°C, the hydrolysis area was clearly expended nearby the reaction spot.

Qualitative reactions in the presence of tributyrin and Tween 80 as substrates (Table 10) revealed that the R2A medium is more suitable for the hydrolysis catalytic reaction of the extracellular lipases secreted by *Psychrobacter* sp. strain.

Table 10. Time dependent hydrolysis diameter

Culture media	The diameter of the hydrolysis zone (cm)	
	3 days of incubation	7 days of incubation
TSA + Tween 1%	0	0,2 (Replicate[1]) 0,2 (Replicate[2])
TSA+ Tributyrin 1%	0	0
R2+Tween 1%	0,2 (Replicate[1]) 0,2 (Replicate[2])	0,7 (Replicate[1]) 0,6 (Replicate[2])
R2+Tributyrin 1%	0	0

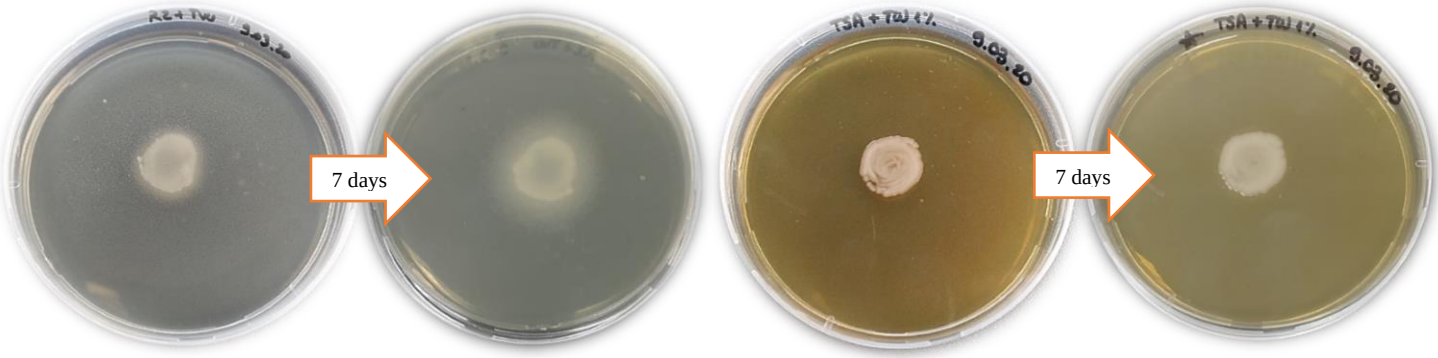

Figure 15. Petri dishes with Tween 80, bacterial strain, on R2A, respectively, TSA culture media.

II.3. Lipolytic activity on vegetal oils

Olive and sunflower oils, in concentrations of 0.5%, 1%, and 1.5% were added to the growth media as a lipase substrate to determine the optimal conditions for extracellular lipase activity. The oils were added to the culture media after the media sterilization. Lipase activity was detected according to the described protocol as red-orange fluorescent halo occurrence due to Rhodamine B input [40].

When using R2A culture media, the highest lipolytic activity of the bacterial strain was observed for a concentration of 1% sunflower oil. However, in the case of TSA medium, a significantly improved activity occurred in the presence of 1.5% sunflower oil (Figure 16), suggesting that this cold-active bacterial strain has a higher lipase activity when using 1.5% sunflower oil concentration. The same high lipolytic activity was appreciated for the highest concentration of the olive oil (1.5%), with a considerable extension around the hydrolysis zone, regardless of the culture media used (Figure 17).

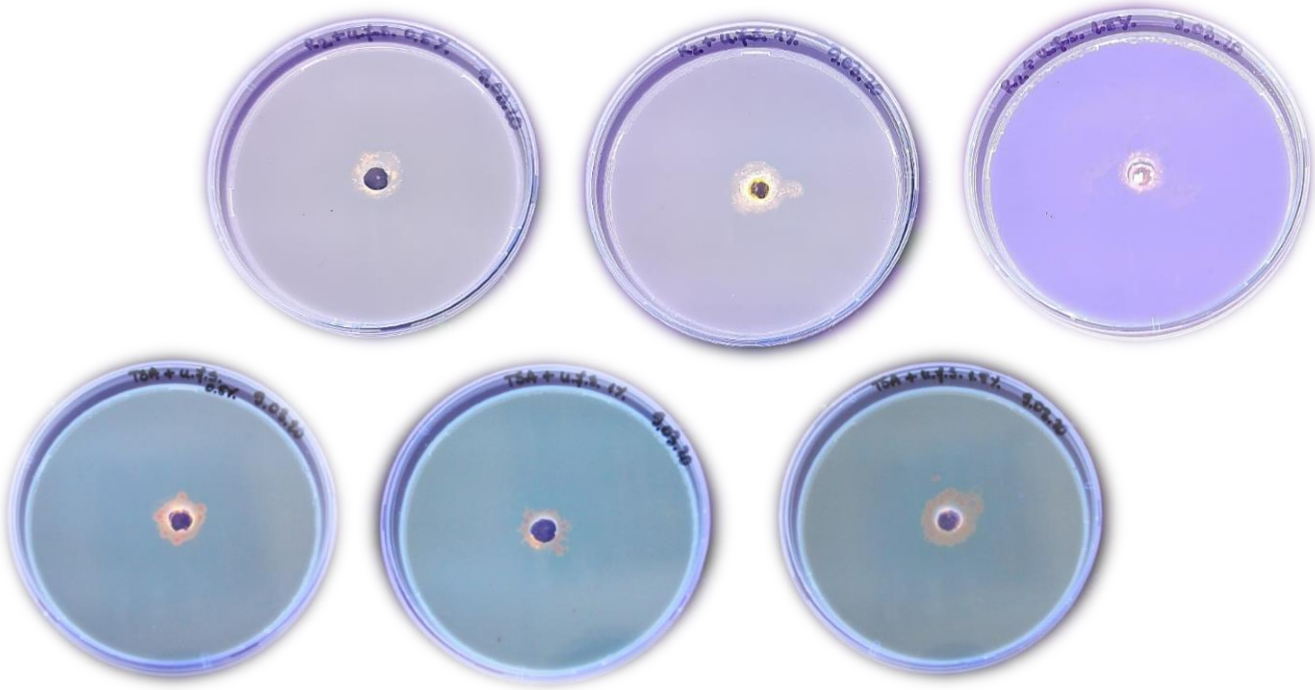

Figure 16. Bacterial growth on R2A (upward), and TSA (downward) media respectively, supplemented with sunflower oil (0.5%, 1%, 1.5%).

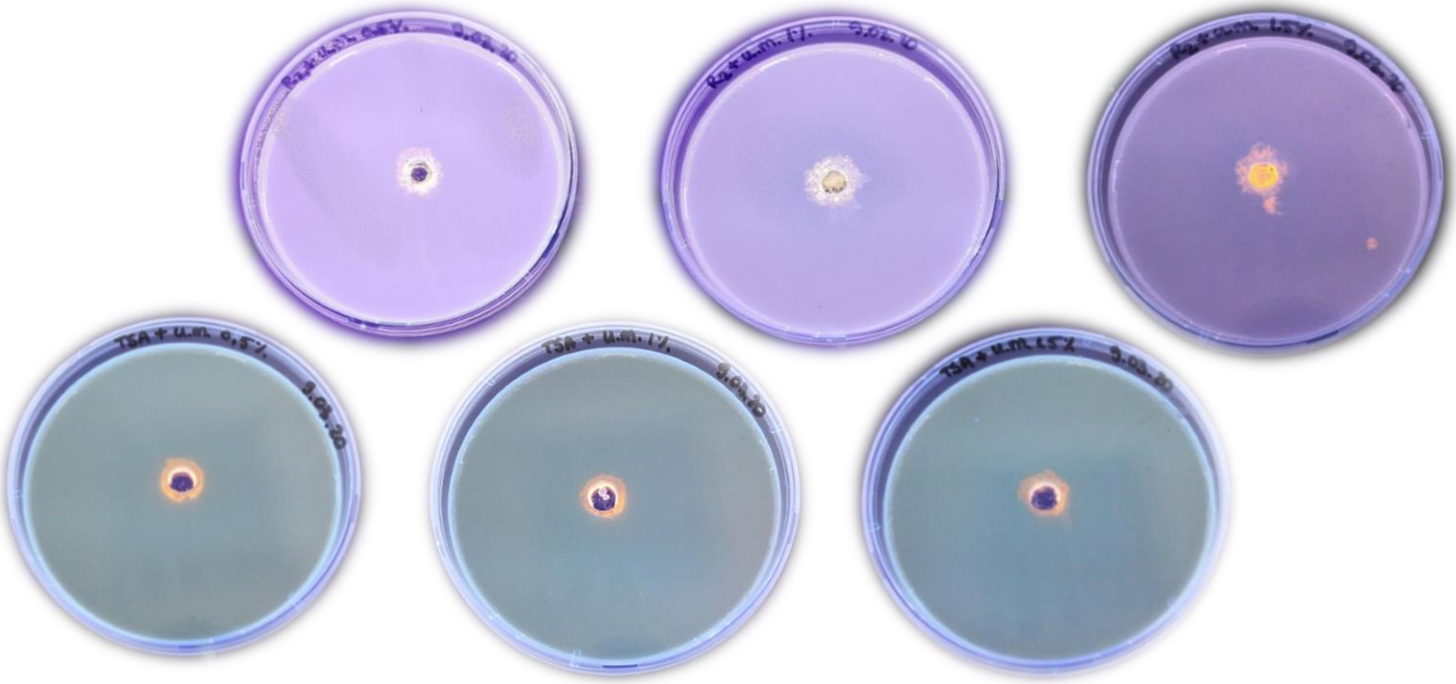

Figure 17. Bacterial growth on R2A (upper) and TSA (lower) culture media supplemented with olive oil (0.5%, 1%, 1.5%)

III. Biocatalyst preparation

III.1.Biocatalyst precipitation

Sistematically, the *Psychrobacter* sp. strain was incubated for 3 days at 15℃ and fully grown cell colonies are able to produce and extracelullarly release proteins into the culture media. As for that, to favour the production of lipases the culture media was initially supplimented with 1% olive oil, as this provides the preferred carbon source for lipolytic hydrolysis.

The culture media is now enriched, assuming the feasible production of extracelular proteins together with lipases of interest. Further, to exclud the intereferents of the media (e.g. nutrients, salts), the total protein was precipitated with 80% acetone, that competes with water molecules linked to the biomolecules, and triggered the precipitation stage. The total protein is obtained as a white powder (Figure 18) and suspended in 100mM TRIS-HCl buffer pH 8.

Figure 18. Precipitation of extracellular protein content of *Psychrobacter* sp. culture medium

For the validation of partially purified protein content obtained after extraction with organic solvent, the extract was measured at 280 nm, and the absorbance value was extrapolated on the calibration curve with bovine serum albumin standards, to estimate the concentration (Figure 19). Sample series of protein precipitate were obtained in the range of 5 – 8 mg/mL.

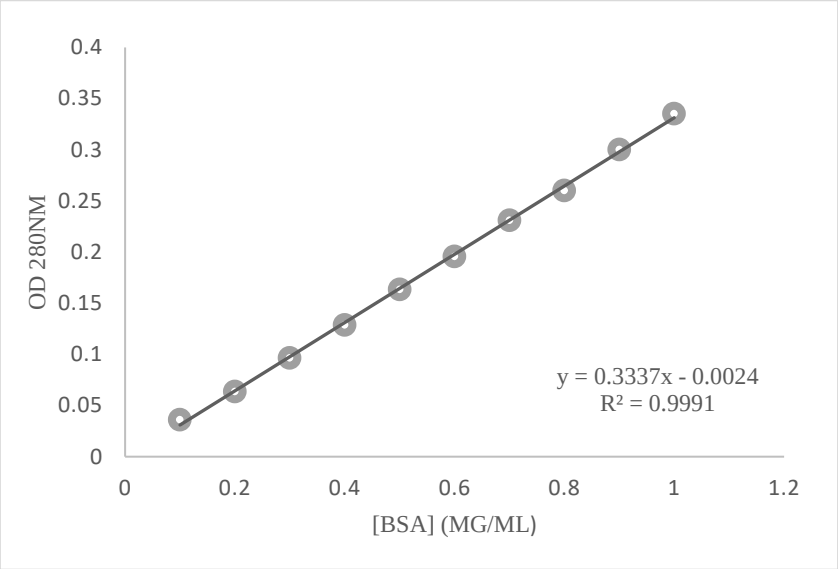

Figure 19. Calibration curve on 0.1 – 1 mg/mL bovin serum albumin (BSA) standards in distilled water.

III.2. Covalent immobilization

III.2.1. Immobilization on modified resin

Covalent immobilization of the enzyme on amino–C_2–methacrylate with glutaraldehyde spacer was firstly performed. The enzyme provides lateral amino groups for linking via –CHO groups, which simultaneously captured the amino groups of the support. After the immobilization procedure, the amount of protein extract left unattached to the support is discriminated by measuring the absorbance of the reaction supernatant, which obviously contains the remained soluble protein fraction. The following performances in Table 11. were obtained after the immobilization procedure:

Table 11. Immobilization capacity of protein extract on amino–C_2–methacrylate.

Starting concentration	Immobilized	Protein loading	Protein recovery
4.96 mg/mL	4.382 mg/mL	41.73 mg protein/g support	88.35%
	4.47 mg/mL	42.33 mg protein/g support	90.12%

As the immobilization results revealed, the reaction in MES buffer was achieved with 90% succes, while for PBS buffered reaction, with 88%. Therefore, good attachement of protein extract on resin beads is accomplished through the above-mentioned protocol (Figure 20.).

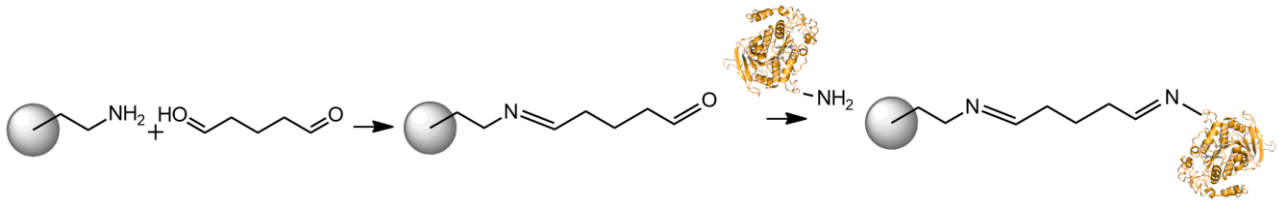

Figure 20. Mechanism of immobilization on amino-C2-metacrylate polymeric beads

III.2.2. Immobilization on magnetic particles

Coated magnetic particles that provide different functional groups on the outer face were tested as supports for the immobilization of the protein extract obtained out of the bacterial culture. There were performed different approaches in the case of the carbodiimide method (Figure 21), the nanosized and microsized magnetic particles with lateral carboxyl groups were diectly treated with EDC activator. A one pot immobilization reaction was also achieved by capturing enzyme carboxyl groups via EDC and linking them further with microsized magnetic beads with lateral amino supply.

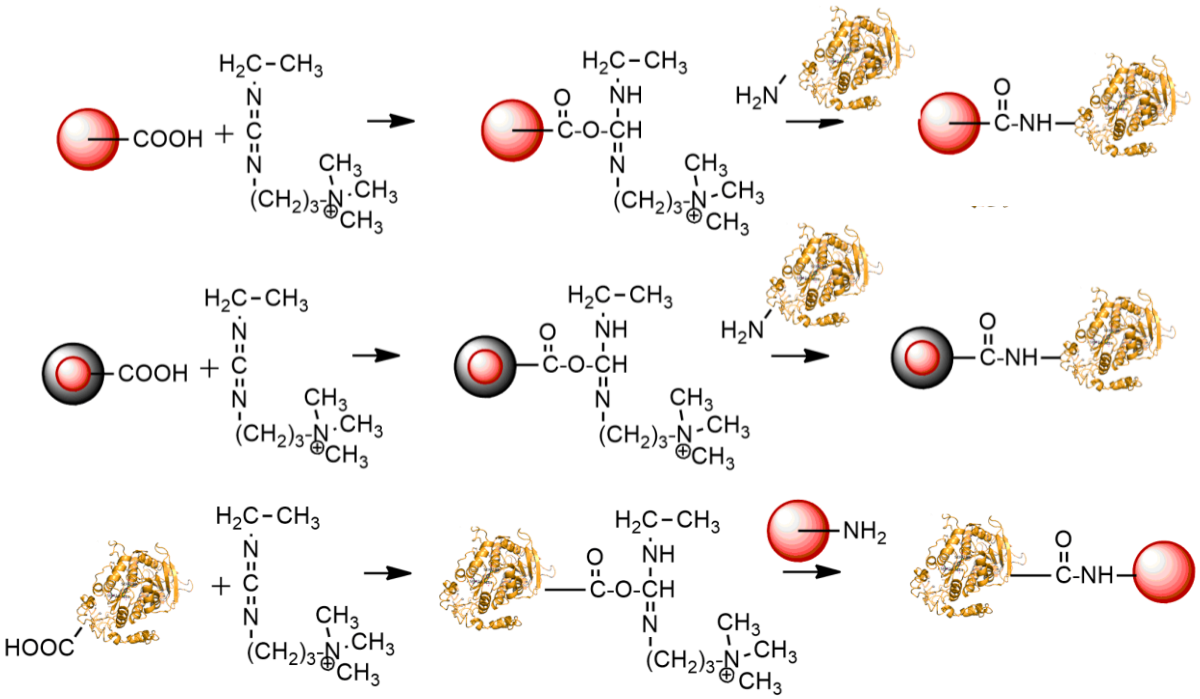

Figure 21. Mechanism of immobilization via carbodiimide methods.

Because the structural analysis agreed to the existence of glycosidic groups for bacterial lipases of classes IV and V, an oxidizing step was introduced prior to immobilization. Sodium periodate targeted the glycosidic groups from lipases and added a plus reactivity by opening the cycle (Figure 22). Magnetic particles providing hydrazine groups ended the immobilization reaction through imine bonds.

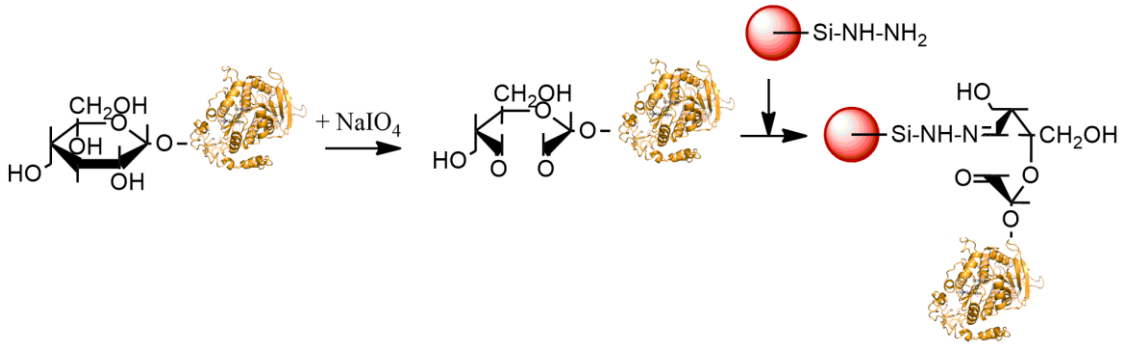

Figure 22. Mechanism of immobilization on Si-MAG-Hydrazine magnetic beads.

The immobilization performance was estimated using UV-analysis at 280 nm against the calibration curve, while the values are listed in Table 12:

Tabel 12. Immobilization capacity of protein extract on different coated magnetic beads.

Starting concentration	**Immobilized on**			
	Si-MAG-Amine	Si-MAG-Carboxyl	Si-MAG-Hydrazine	Fluid-MAG-ARA
6.6 mg/mL	6.55 mg/mL	6.545 mg/mL	6.53 mg/mL	6.33 mg/mL

The performance of the immobilization is similar regardless of the working protocol chosen or the particle matrix. It could be noted that on micro-sized particles the immobilization went with a few percentages better.

IV. Biocatalyst characterization

IV.1. FT-IR analysis

Diffuse Reflectance Infrared Fourier Transform (DRIFT) spectra were measured for free and immobilized support beads. A minimum amount of sample was dilluted with potassium bromide matrix. Amide I band, corresponding to (CO) carbonyl stretching mode of the peptide is present in the region of 1700–1600 cm^{-1}. This band consists of a group of overlapped signals, which contain

information on secondary protein structure of the enzyme. Bands centered at around 1550 cm^{-1} are assignable to the amide II band, which is a out-of-phase combination mode of the NH in plane bend and the CN stretching vibration with smaller contributions from the CO in plane bend and the CC and NC stretching vibrations. Additionally, the peak at 1600 cm^{-1} can be assigned to the asymmetric stretching. Finally, a set of bands can be distinguished in the region of 1400 – 1200 cm^{-1} due to amide III mode. This mode is assigned to the in-phase combination of the NH deformation vibration with CN, with a minor contribution of CO and CC stretching. These polypeptide bands are complex and do not allow a direct correlation with the protein structure mode of carboxylic groups, (COO), of aspartic acid (Asp A.) and/or glutamic acid (Glu A.) in side chain. α-Helices show a strong and characteristic absorption band centered at 1660 cm^{-1}. Additionally, it is also possible to identify a band at 1645 cm^{-1}, which can be assigned to random structures, such as turns and coil specific for cold-active proteins. β-Sheets have two signals at ~1635 (intense) and ~1683 cm^{-1} (weak), but not distinguishable in this case. The splitting of the amide I mode in β-sheets structures is a consequence of differences in hydrogen-bridged bonds and the dipole transition coupling. The band at 1683 cm^{-1} may also contain overlapping contributions (i.e. that could not be resolved in our spectra) due to turn structures [49, 50].

It is clear that the immobilization was succesfully achieved via covalent linking of the biomaterial to amino-C_2-metacrylate support given the interferogram (Figure 23). For the immobilized specimen, the specific bands of amide I and II around 1600 – 1700 cm^{-1} are well distinguished, as coming from the peptide bonds provided by the protein. The support, as being a croslinking metacrylate polymer with amino- disposable groups, has a specific band at 1730 cm^{-1} as C=O stretching carboxyl for methacrylate, as well as 2 peaks between 3300 and 3500 cm^{-1} signing for primary amino groups projecting out by the outer face of the polymer.

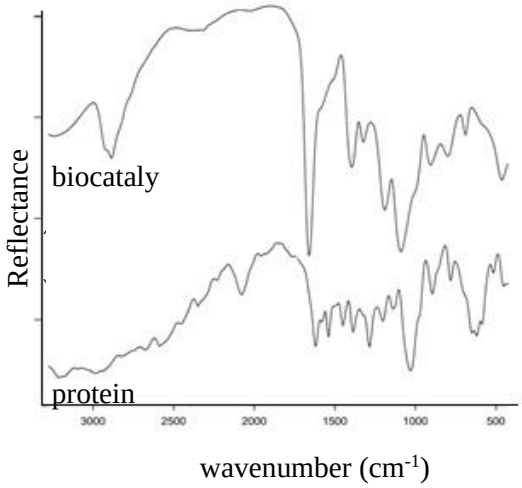

Figure 23. DRIFT spectra of protein and MTC-NH_2 biocatalyst.

FTIR spectra of magnetite exhibit two strong infrared absorption bands at 570 and 390 cm^{-1}. According to Ishii and Nakahira, these bands can be assigned to the Fe–O stretching mode of the tetrahedral and octahedral sites (the band at 570 cm^{-1}) and to the Fe–O stretching mode of the octahedral sites (the band at 390 cm^{-1}). Maghemite, a defective form of magnetite, has absorption bands at 630, 590 and 430 cm^{-1} [51]. The strong asymmetrical band at 578 cm^{-1} characteristic to Fe–O stretching vibrations includes also the Fe–OH vibration band located at 630 cm^{-1} and possible Fe–O vibration bands of maghemite (635 cm^{-1}) [51].

Important to be considered is that for the immobilization performance, the bands for amide I, II and III are evidenced, while specific sharp peaks are located in the low wavenumber region for the support evidence (Figure 24 – 27). In biological materials and protein spectra, large bands in the region of large wavenumbers are clearly related to OH streching groups, as the water trances could not be overcome.

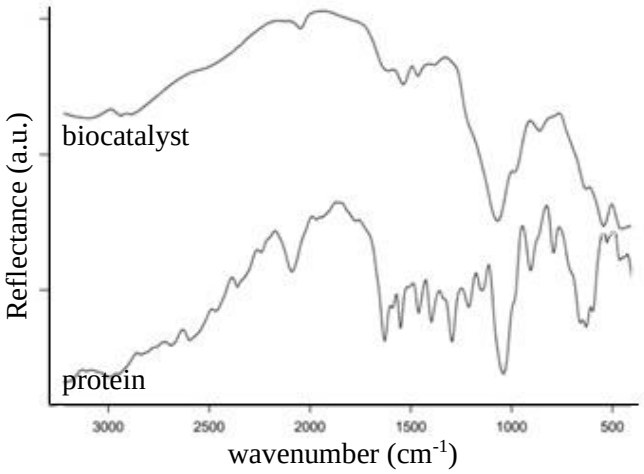

Figure 24. DRIFT spectra of protein and sMP-NH-NH_2 bc.

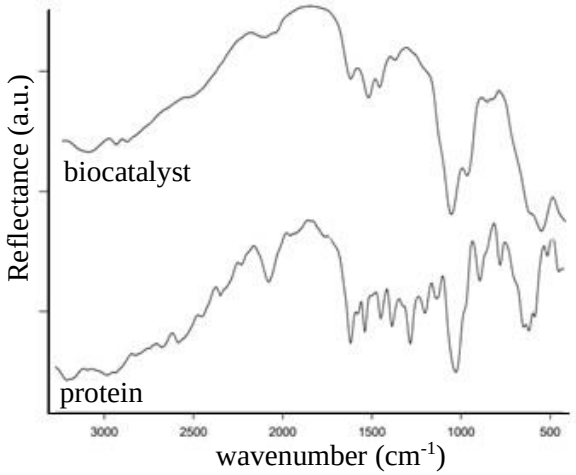

Figure 25. DRIFT spectra of protein and sMP-NH_2 bc.

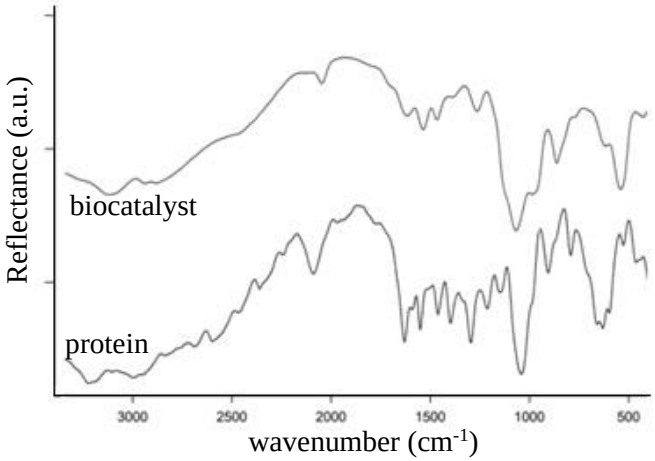

Figure 26. DRIFT spectra of protein and fMP-COOH bc.

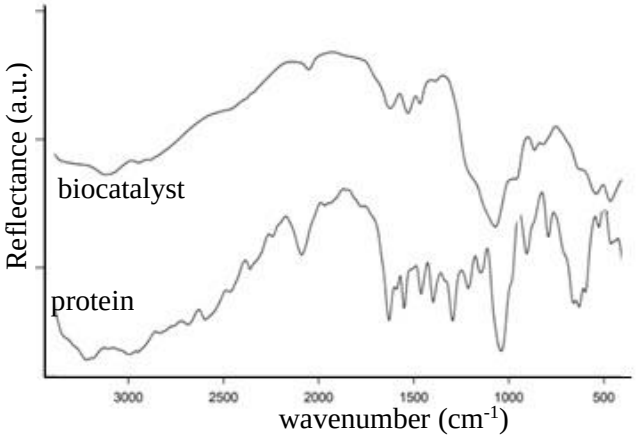

Figure 27. DRIFT spectra of protein and sMP-COOH bc.

IV.2. SEM analysis

The following micrographs were performed by Surface Electron Microscopy on biocatalyst specimens to highlight the immobilization of the protein content on the functionalized surface of the support particles. The appearance of magnetic particles is defined and characteristically crystallized for magnetite and maghemite. In the case of the free support based on methacrylate polymer, the beads have a clear, smooth aspect. The analysis of the immobilized specimen intervenes with the change in the morphology of the magnetic crystals or in the smoothness of the resin beads. A lighter contrast highlights the protein deposits that adhere covalently to the support surface. The analysis involved *a priori* metallization with gold (Figure 28 – 32).

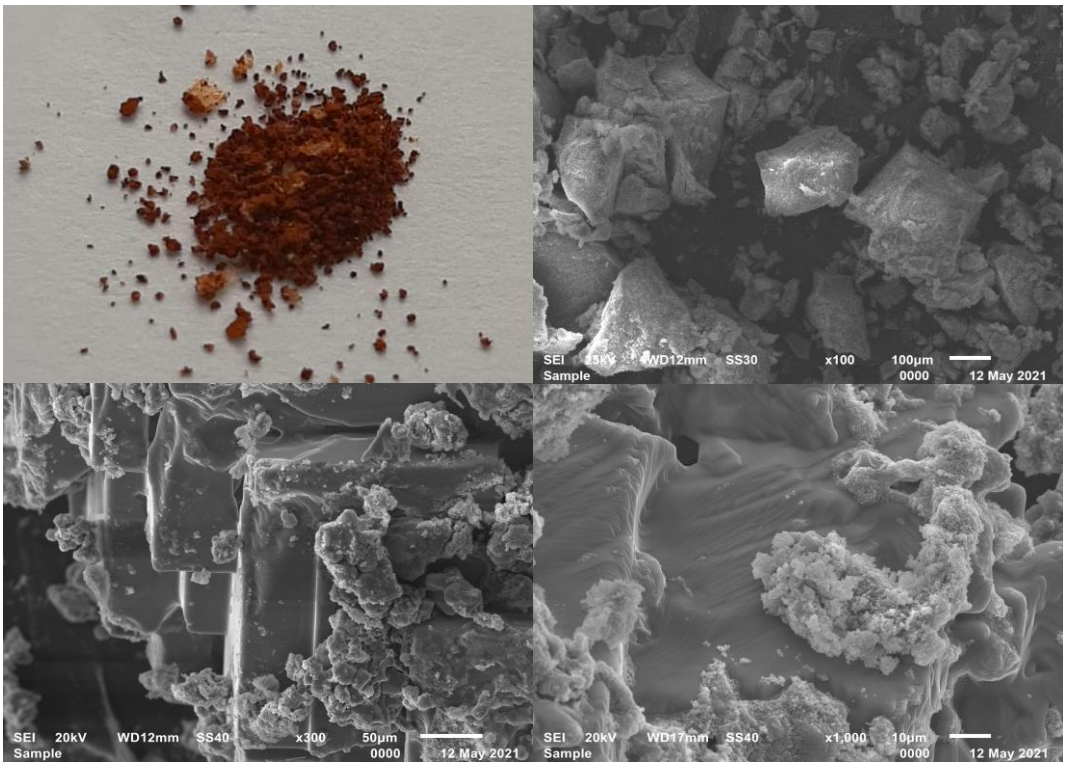

Figure 28. A. Real evidence of sMP-COOH material. SEM micrographs: B. Free support, C. Immobilized-protein support (50 µm), D. Immobilized-protein support (10 µm).

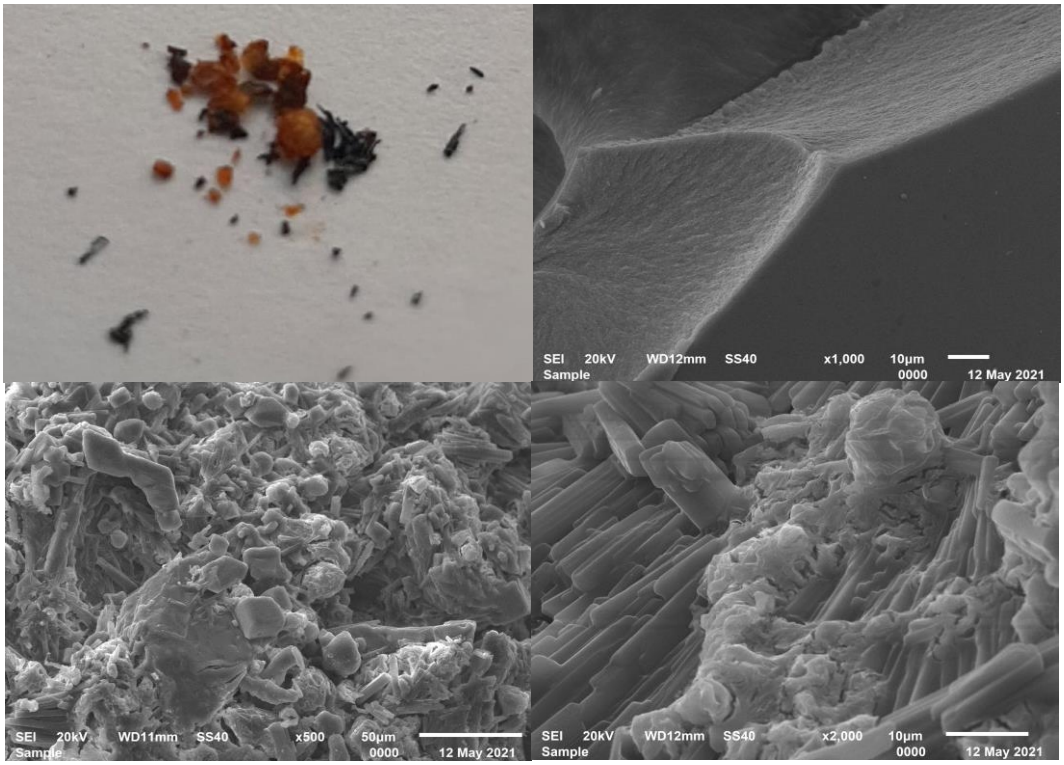

Figure 29. A. Real evidence of fMP-COOH material. SEM micrographs: B. Free support, C. Immobilized-protein support (50 µm), D. Immobilized-protein support (10 µm).

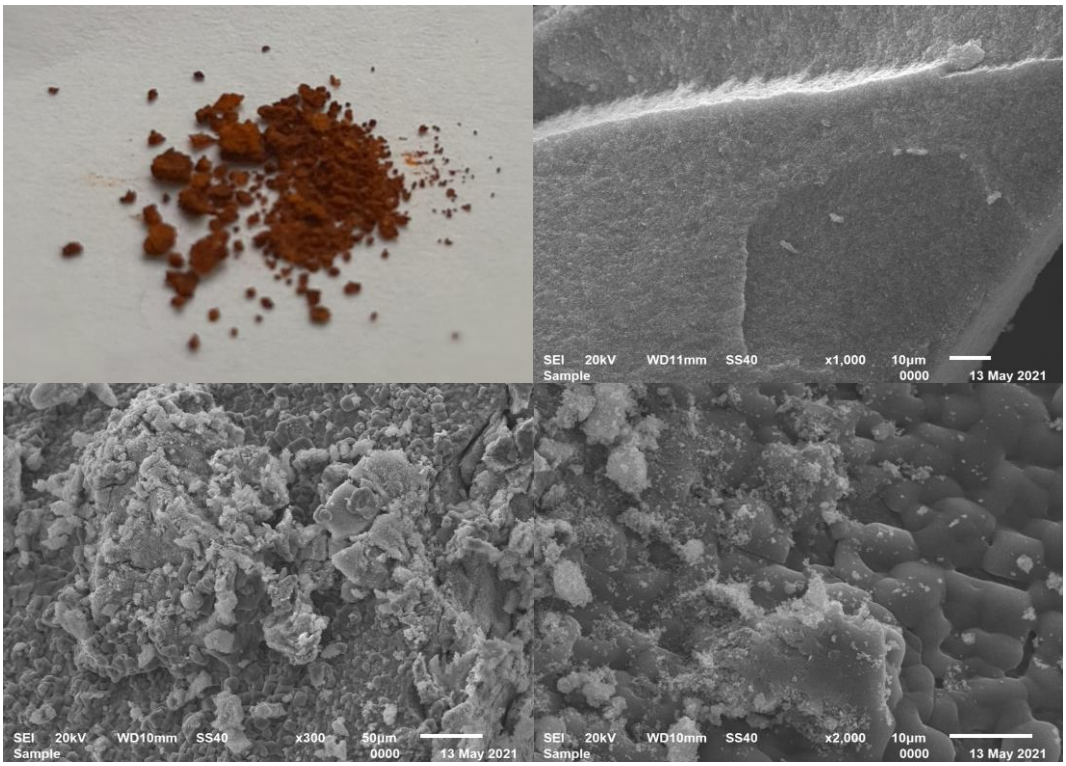

Figure 30. A. Real evidence of sMP-NH_2 material. SEM micrographs: B. Free support, C. Immobilized-protein support (50 µm), D. Immobilized-protein support (10 µm)

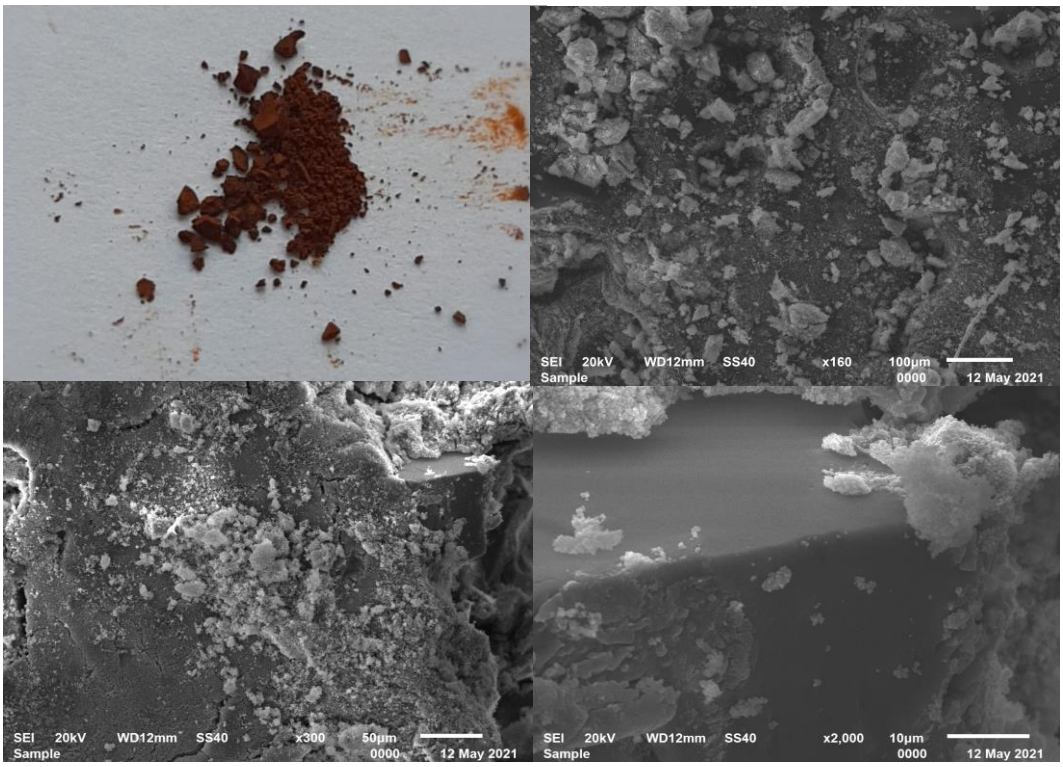

Figure 31. A. Real evidence of sMP-NH- NH_2 material. SEM micrographs: B. Free support, C. Immobilized-protein support (50 µm), D. Immobilized-protein support (10 µm)

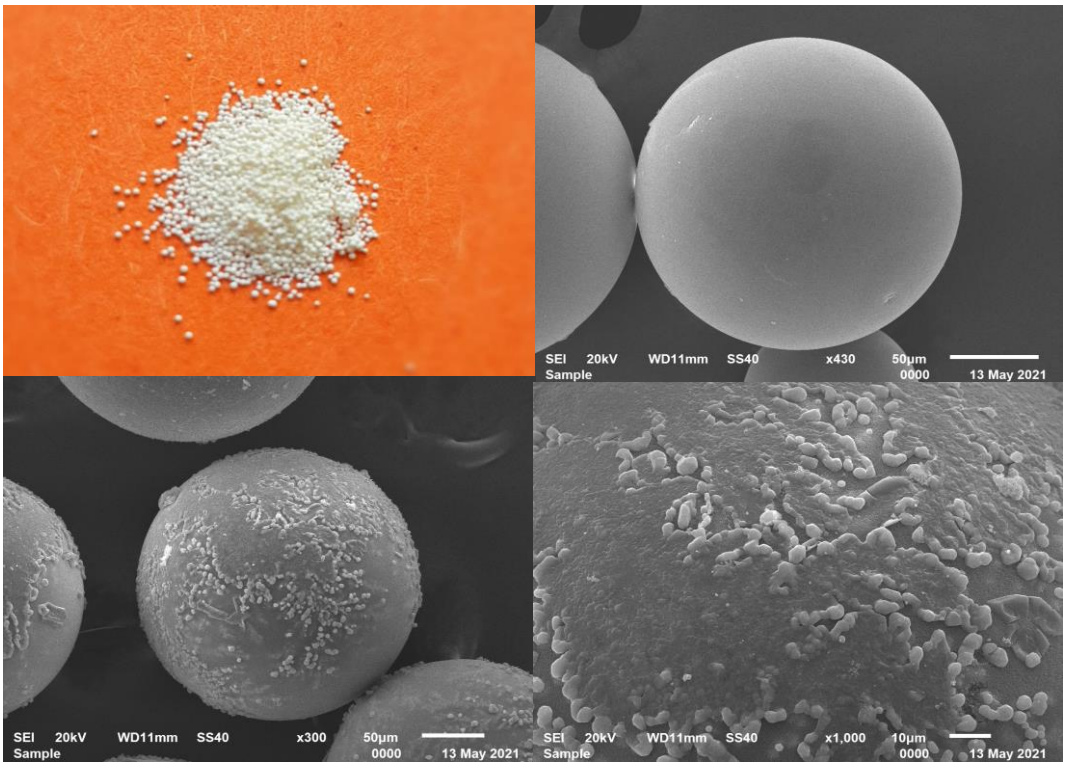

Figure 32. A. Real evidence of MTC- NH_2 material. SEM micrographs: B. Free support, C. Immobilized-protein support (50 µm), D. Immobilized-protein support (10 µm)

IV.3. Enzyme activity

The system for lipase activity implies the formation of fatty acids in an aques solution, as in other terms a not clear, but a dispersed solution is continuously formed during the enzymatic reaction. For this reason, a discontinuous kinetics is approved in the literature for measuring the lipase activity, as the formation of acid product is measured after 30 minutes, and activity is reported in terms of concentration per min against the calibration curve obtained with different known substrate concentrations (Figure 33). Moreover, the classical pathway for hydrolysis happened at 37°C, while in this study the reaction at 25°C was introduce to evaluate the cold-active character of lipases.

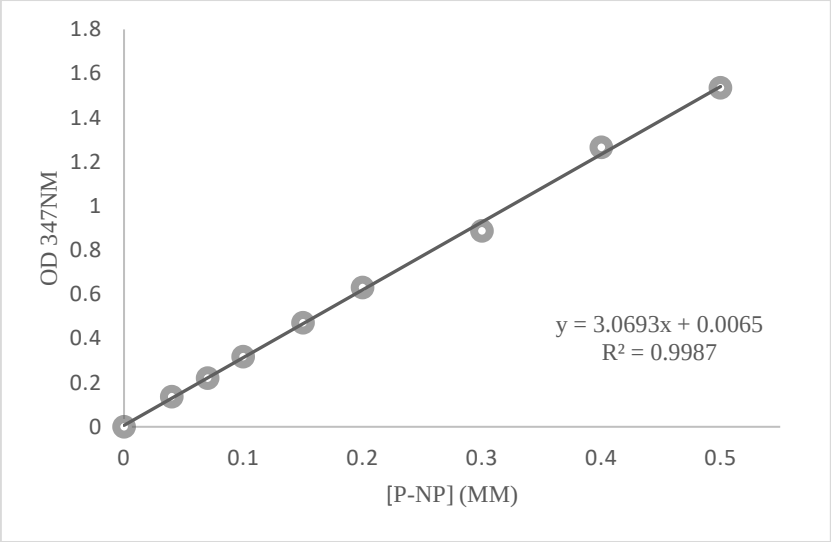

Figure 33. Calibration curve on 0 – 0.5 mM p-nitrophenol standards in ethanol.

On the p-nitrophenol butyrate substrate of different concentrations, activity measurements were performed according to the protocol. By plotting Lineweaver-Burk were calculated the kinetic constants Km and Vmax, and particularly kcat, for two reaction temperatures (Figure 34). According to the Km values, the cold-active character of the lipases is maintained with the increase of the temperature by up to 15 degrees in addition, compared to the optimum T estimated at 25°C, without substantial changes of the characteristic lipolytic activity. In the case of the catalytic constant, similar values are recorded for both temperatures.

Catalytic efficiency was calculated as the ratio between kcat / Km. The close values of the ratio for both temperatures support the structural and functional stability of the proteinaceous material. An at least interesting observation is in the case of the specimen immobilized on magnetic nanoparticles, where the catalytic efficiency proves to be the most promising.

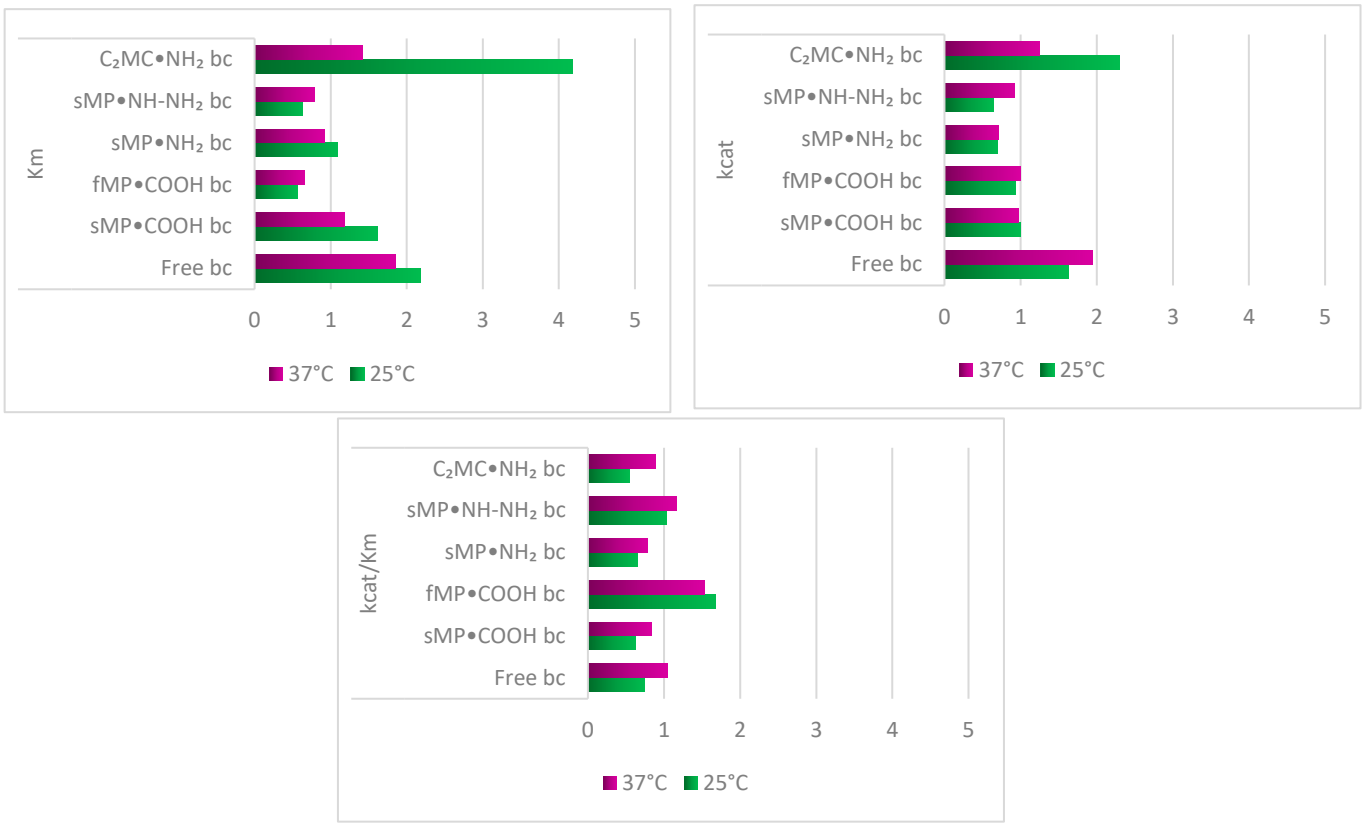

Figure 34. Lipolytic activity for all biocatalysts on p-nitrophenyl butyrate substrate.

V. Biocatalyst performance

V.1. Design of the biocatalytic system

The biocatalytic system was composed based on the main idea on which the thesis is founded, namely, the valorization of silymarin. Starting from one of the most biologically active compounds of silymarin, e.g., silybin, esterification reactions were directed to its hydroxyl groups of aromatic and alcoholic origin. Experiments were performed both with fatty acids (octanoic acid, oleic acid) for esterification reaction, but also with fatty acid esters (methyl decanoate, methyl laurate, methyl myristate, methyl palmitate) via transesterification. A useful comparison could be outlined by using the free and immobilized protein material involved in catalyzing the reaction. Given the origin of the protein extract from the extremophilic strain of *Psychrobacter* sp., the reaction temperature was set to 25°C.

Given the HPLC-DAD analysis, unreacted substrates were constantly identified against standards as having the following retention times: silybin at 2.4 minutes, octanoic acid at 2.9 minutes, oleic acid at 3.7 minutes, methyl decanoate at 3.1, methyl laurate at 3.3, methyl myristate at 3.7,

methyl palmitate at 4.1 minutes, respectivly. The process performance was related to each calculated value obtained in terms of substrate conversion for every synthesis, by using the well-know formula:

$$C(\%) = \frac{\text{mass of converted silybin}}{\text{initial mass of silybin}} \cdot 100$$

V.2. Optimization of system parameters

Raw culture media vs. Protein precipitate

The culture medium contains multiple interferences that imprint nonspecific peaks on the control chromatograms for the reaction of interest. At the same time, the culture medium was supplemented with 1% olive oil to increase the extracellular lipase production, and this may work towards side reaction of hydrolysis or synthesis from the oil supplement. The protein precipitate rises to the desired performance, with a good differentiation of the product peaks and unreacted substrate.

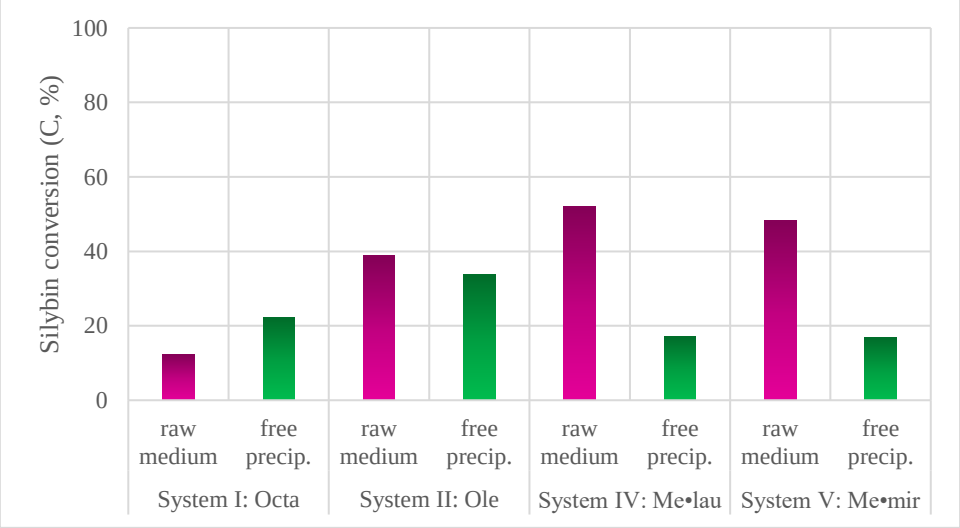

Figure 35. System performance in terms of silybin conversion by using raw culture media vs. protein precipitate.

Free biocatalyst performance at 25°C or 40°C

Knowing that the biocatalyst is cold-active, its catalytic potential is expected to be at low temperatures. However, the results in terms of substrate conversion involve higher values at 40°C. One possible explanation is that the lipase biocatalyst is stable even with increasing temperature, having considerable residual catalytic activity. At the same time, the esterification reaction may be stimulated by the increase of temperature and esters could be formed uncatalyzed. For this reason and for the evaluation of the biocatalyst at its potential, the system temperature remains settled at 25°C.

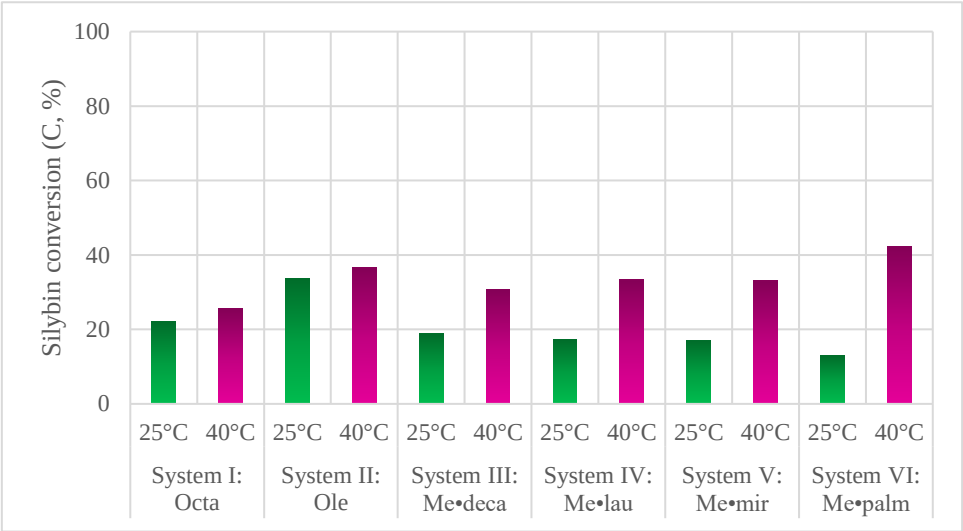

Figure 36. System performance in terms of silybin conversion by using different temperature with free biocatalyst

Immobilized biocatalyst at 25°C or 40°C

An increased performance of the biocatalytic system is desired to support the esterification of silybin and to contribute to the improvement of the liposolubility properties of silymarin. Preliminary testing of the immobilized biocatalytic material involved the use of the support based on polymer resin at 2 temperatures. It is observed that the cold-active potential of the proteinaceous material is supported by its immobilization, as lipases tend towards an increased catalytic activity when adhere between two heterogeneous media, in this case the support and the liquid medium of the reaction. At the same time, for the temperature of 25°C, the best conversion values are obtained, another evidence of the cold-active catalytic character storage.

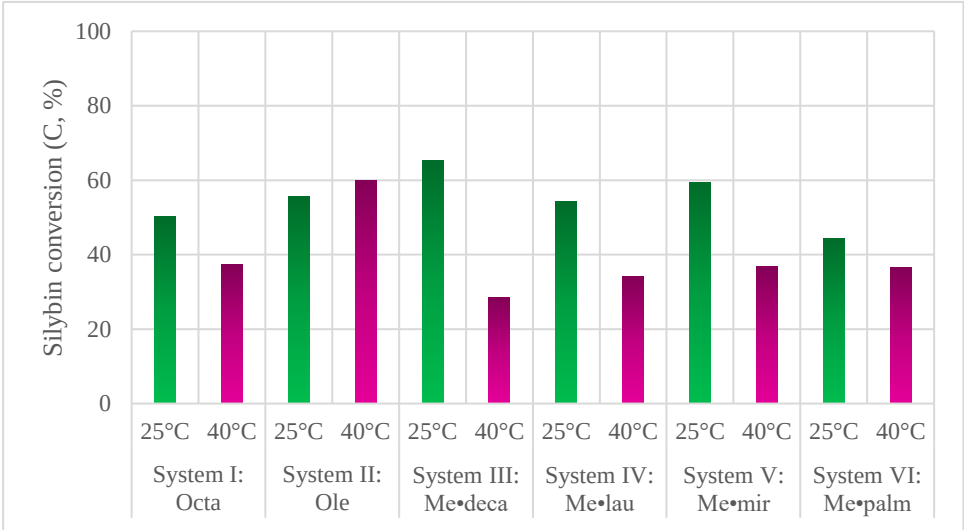

Figure 36. System performance in terms of silybin conversion by using different temperature with MTC-NH_2 immobilized biocatalyst.

V.3. Evaluation of the biocatalysts

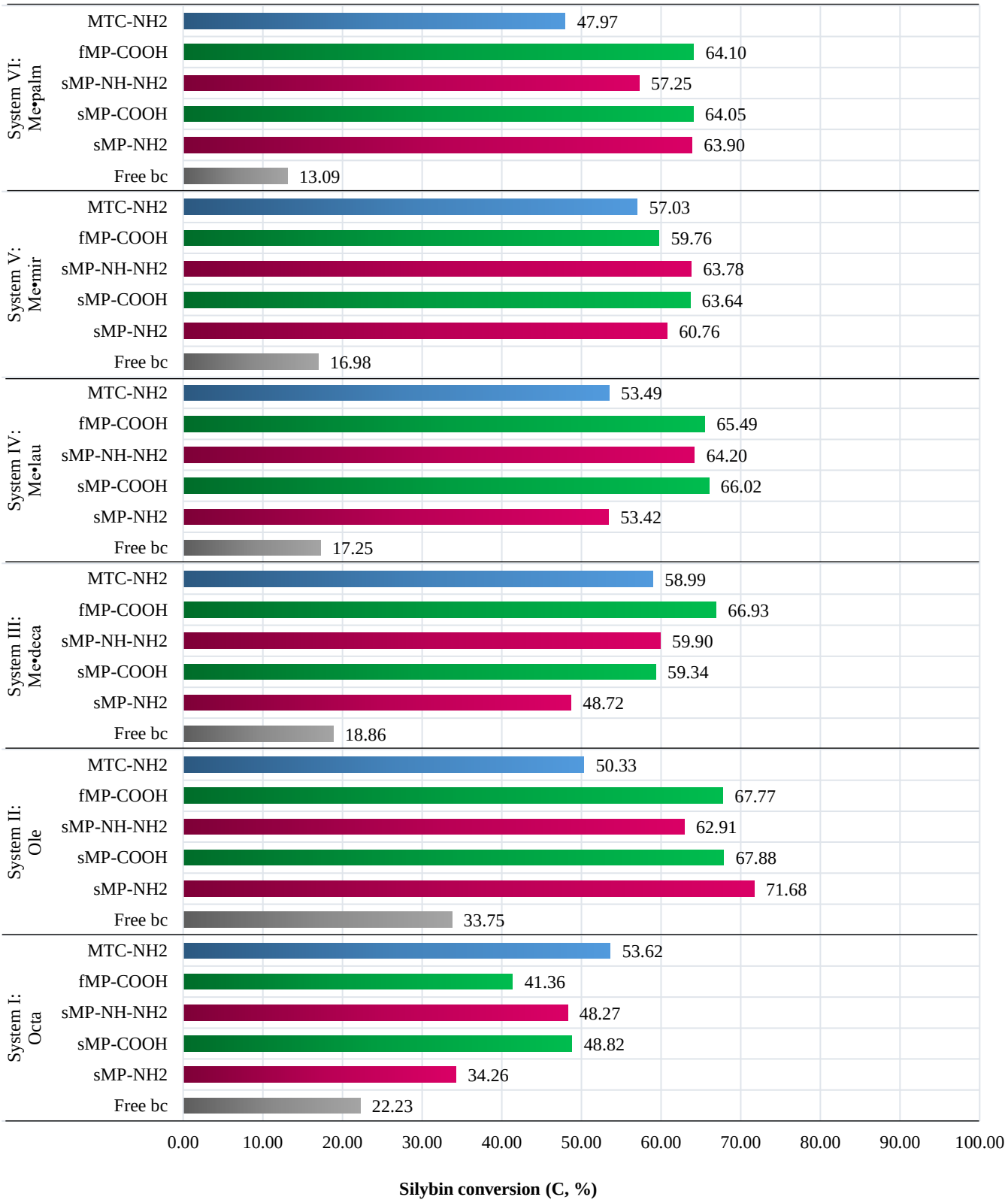

Figure 37. System performance in terms of silybin conversion for every biocatalyst specimen

Following the screening performed on the biocatalytic systems proposed for the esterification of silybin with different fatty acids, 3 questions arise:

a) Why does the free biocatalyst have a lower performance than the immobilized biocatalyst?

b) Why after immobilization the lipases adhering to the support show an improved catalytic activity?

c) What is the most promising immobilized biocatalyst for the esterification process?

With these nuances in mind, one could evade very useful observations and information.

In the case of the free biocatalyst, the performance range in terms of substrate conversion varies between 13 and 34%. The conversion values decrease in the case of the free biocatalyst, with the increase of the hydrocarbon chain of the acylating agent: 34% for the oleic acid system, 13% for the methyl palmitate system. It is true that being a total protein content embedded generically in the free biocatalyst, steric hindrances are a risky factor in achieving the synthesis, the lipase catalytic lid being restricted by the neighboring interactions.

In the case of the immobilized biocatalyst, the performance range varies between 41 and 66%. There is no decisive trend for the behavior of immobilized biocatalysts, but a first important observation is based on a catalytic activity improved by several tens of percent compared to the free biocatalyst. Thus, by immobilization even though covalent, protein stability is sustained. It is approved in the scientific community that lipases have an unusual behavior, but very beneficial when they are found at the interface between two different environments. Most studies are based on interfacial activation between organic and aqueous medium. In the present case, the heterogeneity of the system is given by the immobilized form and the liquid reaction medium.

A second observation correlated with the immobilized biocatalyst is given by the increased biocatalytic potential in a constant trend with the increase of the hydrocarbon chain coming from the acylating agent. Basically, the protein conformation sustained by immobilization allows the facial reception of the substrate at the catalytic site.

It is easy to notice that the immobilized catalysts have similar performance values, considering the functionality of each support and the immobilization method used, for each individual biocatalytic system. Thus, there is no major difference that can serve as a conclusion for a particular biocatalyst. However, globalizing this study, values of 65% (excluding the octanoic acid system) were obtained with the biocatalyst based on nanoparticle support.

CONCLUSIONS

REFERENCES

[1]. Flora, K., Hahn, M., Rosen, H., Benner, K., *Milk Thistle (Silybum marianum) for the Therapy of Liver Disease*. AJG, 93 (**1998**), 139-143.

[2]. Duran, D., Otles, S., Karasulu, E., *Determination Amount of Silymarin and Pharmaceutical Products from Milk Thistle Waste Obtained from Cold Press*. Acta Pharmaceutica Sciencia, 57 (**2019**), 85-101.

[3]. Begum, S. A., Sahai, M., Ray, A. B., *Non-convetional Lignans: Coumarinolignans, Flavonolignans, and Stilbenolignans*, Springer-Verlag/Wien, **2010**, Chapter 3. Flavonolignans, pg. 29-48.

[4]. Csupor, D., Csorba, A., Hohmann, J., *Recent advances in the analysis of flavonolignans of Silybum marianum.* Journal of Pharmaceutical and Biomedical Analysis, 130 (**2016**), 301-317.

[5]. Vastalova, J., Tinkova, E., Biedermann, D., Kosina, P., Ulrichova, J, Svobodova, A.R., *Skin Protective Activity of Silymarin and its Flavonolignans*. MDPI Journal- Molecules, 24 (**2019**), 1022.

[6]. Di Costanzo, A., Angelico, R., *Formulation Strategies for Enhancing the Bioavailability of Silymarin: The State of the Art.* MDPI Journal-Molecules, 24 (**2019**), 2155.

[7]. Drouet, S., Doussot, J., Garros, l., Mathiron, D., Bassard, S., Favre-Reguillon, A., Molinie, R., Laine, E., Hano, C., *Selective Synthesis of 3-O-Palmitoyl-Silybin, a New-to-Nature Flavonolignan with Increased Protective Action against Oxidative Damages in Lipophilic Media.* MDPI Journal-Molecules, 23 (**2019**), 2594.

[8]. Theodosiou, E., Purchartova, K., Stamatis, H., Kolisis, F., Kren, V., *Bioavalability of silymarin flavonolignans: drug formulations and biotransformation*. Phytochem Rev, (**2013**).

[9]. Fidrus, E., Ujhelyi, Z., Feher, P., Hegedus, C., Janka, E. A., Paragh, G., Vasa, G., Bacskay, I., Remenyik, E., *Silymarin: Friend or Foe of UV Exposed Keratinocytes?*, MDPI-Molecules, 24 (**2019**), 1652.

[10]. Chambers, C.S., Biedermann, D., Valentova, K., Petraskova, L., Viktorova, J., Kuzma, M., Kren, V., *Preparation of Retinoyl-Flavonolignan Hybrids and Their Antioxidant Properties*. MDPI Journal-Antioxidants, 8 (**2019**), 236.

[11]. Duan, L., Carrier, D.J., Clausen, E.C., *Silymarin Extraction from Milk Thistle Using Hot Water. Applied Biochemistry and Biotechnology*, 113-116 (**2004**)

[12]. Bijak, M., *Silybin, a Major Bioactive Component of Milk Thistle (Silybum marianum L. Gaernt.)-Chemistry, Bioavailability, and Metabolism*, MDPI-Molecules, 22 (**2017**), 1942.

[13]. Tufvesson, P., Fu, W., Jensen, J. S., Woodley, J. M., *Process considerations for the scaleup and implementation of biocatalysis*, Food and Bioproducts Processing, 88 (**2010**) 3-11.

[14]. Tufvesson, P., Lima-Ramos, J., Nordblad, M., Woodley, J. M., *Guidelines and Cost Analysis for Catalyst Production in Biocatalytic Processes*, Organic Process Research & Development, 15 (**2011**) 266-274.

[15]. Santacoloma, P. A., Sin, G., Gernacy, K., V., Woodley, J. M., *Multienzyme-Catalyzed Processes: Next-Generation Biocatalysis*, Organic Process Research & Development, 15 (**2011**) 203-212.

[16]. Santiago, M., Ramirez-Sarmiento, C.A., Zamora, R.A., Parra, L.P., *Discovery, Molecular Mechanisms and Industrial Applications of Cold-Active Enzymes*. Frontiers in Microbiology, 7 (**2016**), 1408.

[17]. Brenchley, JE, *Psychrophilic microorganisms and their cold-active enzymes*, Journal of Industrial Microbiology, 17 (**1996**), 432-437.

[18]. Mangiagalli, M., Brocca, S., Orlando, M., Lotti, M., *The cold revolution. Present and future applications of cold-active enzymes and ice-binding proteins*. New Biotechnology, 55 (**2020**), 5-11.

[19]. Hackett, E. S., Twedt, D.C., Gustafson, D.L., *Milk Thistle and Its Derivative Compounds: A review of opportunities for Treatment of Liver Disease*, J Vet Intern. Med., 27 (**2013**), 10-16.

[20]. Cavicchioli, R., Siddiqui, K., Andrews, D., Sowers, K. R., *Low-temperature extremophiles and their applications*, Current Opinion in Biotechnology, 13 (**2002**), 253-261.

[21]. Kovacic, F., Babic, N., Krauss, U., Jaeger, K.E., *Classification of Lipolytic Enzymes from Bacteria*. Research Gate, (**2019**).

[22]. Konwar, B.K., Sagar, K., Lipase. *An Industrial Enzyme Through Metagenomic*s, Apple Academic Press, NJ, **2018**, Chapter 1.6. Classification of Bacterial Lipolytic Enzymes, pgs. 16-20.

[23]. Kavitha, M., *Cold active lipases-an update*, Frontiers in Life Science, **2016**.

[24]. Gandhi, N. N., Patil, N., Sawant, S. B., Joshi, J. B., Wangikar, P. P., Mukesh, D., *Lipase-Catalyzed Esterification*, Catal. Rev.- Sci. Eng., 42 (**2000**), 439-480.

[25]. De Maria, P., D., Carboni-Oerlemans, C., Tuin, B., Bargeman, G., van der Meer, A., van Gemert, R., *Biotechnological applications of Candida antarctica lipase A: State-of-the-art*, Journal of Molecular Catalysis B: Enzymatic, 37 (**2005**), 36-46.

[26]. Stergiou, P.-Y., Foukis, A., Filippou, M., Koukouritaki, M., Parapouli, M., Theodorou, L. G., Hatziloukas, E., Afendra, A., Pandey, A., Papamichael, E. M., *Advances in lipase-catalyzed esterififcation reactions*, Biotechnology Advances (**2013**).

[27]. Spector, A. A., *Essentiality of Fatty Acids*, Lipids, 34 (**1999**), 51-53.

[28]. Lawerence, G. D., *The Fats of Life. Essential Fatty Acids in Health and Disease*, Rutgers University Press, **2010**, Chapter 2, 15-20.

[29]. Das, U. N., *Essential fatty acids: biochemistry, physiology and pathology*, Biotechnol. J., 1 (**2006**), 420-439.

[30]. Lee, C.W., Jang, S.H., Chung, H.S., *Improving the Stability of a Cold-Adapted Enzymes by Immobilization*. MDPI Journal-Catalysts, 7 (**2017**), 112.

[31]. Vaghari, H., Jafarizadeh-Malmiri, H., Mohammadlou, M., Berenjian, A., Anarjan, N., Jafari, N., Nasiri, S., *Application of magnetic nanoparticles in smart enzyme immobilization*, Biotechnol. Lett., 38 (**2016**), 223-233.

[32]. Xie, W., Ma, N., *Enzymatic transesterification of soybean oil by using immobilized lipase on magnetic nano-particles*, Biomass and Bioenergy, 34 (**2010**), 890-896.

[33]. Gasteiger, E., Hoogland, C., Gattiker, A., Duvaud, S., Wilkins, M.R., Appel, R.D., Bairoch, A., *The Proteomics Protocols Handbook*, Humana Press Inc., Totowa, NJ, **2005**, Chapter 52. Protein Identification and Analysis Tools on the ExPASy Server, pgs. 571-607.

[34]. Needleman, S.B., Wunsch, C.D., *A general method applicable to the search for similarities in the amino acid sequence of two proteins*, J. Mol. Biol. (**1970**), 48(3):443-53.

[35]. Sievers, F., Wilm, A., Dineen, D., Gibson, T.J., Karplus, K., Li, W., Lopez, R., McWilliam, H., Remmert, M., Söding, J., Thompson, J.D., Higgins D.G., *Fast, scalable generation of high-quality protein multiple sequence alignments using Clustal Omega*, Mol. Syst. Biol. (**2011**), 7:539.

[36]. Ashok Kumar, T., *CFSSP: Chou and Fasman Secondary Structure Prediction server*, Wide Spectrum: Research Journal (**2013**), 1(9):15-19.

[37]. Yang, J., Yan, R., Roy, A., Xu, D., Poisson, J., Zhang, Y., *The I-TASSER Suite: Protein structure and function prediction.* Nature Methods (**2015**), 12(1):7-18.

[38]. Juni, E., *The Prokaryotes*, Springer Science+Business Media, New York, **1992**, Chapter 174. The Genus Psychrobacter, pgs. 3242-3246.

[39]. Kouker, G., Jaeger, K.E., *Specific and Sensitive Plate Assay for Bacterial Lipases*, Applied and Environmental Microbiology (**1987**), 53: 211-213.

[40]. Ramnath, L., Sithole, B., Goviden, R., *Identification of lipolytic enzymes isolated from bacteria indigenous to Eucalyptus wood species for application in the pulping industry*. Biotechnology Reports (**2017**), 15:114-124.

[41]. Illanes, A., *Enzyme Biocatalysis*, Springer, **2008**, Cap. 6.3. Chimioselective Esterification of Wood Sterols with Lipases, pg. 292-308.

[42]. Neagu, S., Preda, S., Anastasescu, C., Zaharescu, M., Enache, M., Cojoc, R., *The functionalization of silica and titanate nanostructures with halotolerant proteases*, Rev. Roum. Chim., 59 (**2014**), 97-103.

[43]. Lite, C., Ion, S., Tudorache, M., Zgura, I., Galca, A., C., Enache, M., Maria, G., M., Parvulescu, V.I., *Alternative lognopolymer-based composites useful as enhanced functionalized support for enzymes immobilization*, Catalysis Today, In press (**2020**).

[44]. Xuezheng, L., Shuoshuo, C., Guoying, X., Shuai, W., Ning, D., Jihong, S., *Cloning and heterologous expression of two cold-active lipases from the Antarctic bacterium Psychrobacter sp. G*. Polar Research (**2010**), 29:421-429.

[45]. Novototskaya-Vlasova, K., Petrovskaya, L., Yakimov, S., Gilichinsky, D., *Cloning, purification and characterization of a cold-adapted esterase produced by Psychrobacter cryohalolentis K5T from Siberian cryopeg*. FEMS Microbiol Ecol (**2012**), 2:1-9.

[46]. Santiago, M., Ramirez-Sarmiento, C.A., Zamora, R.A., Parra, L.P., *Discovery, Molecular Mechanisms and Industrial Applications of Cold-Active Enzymes.* Frontiers in Microbiology, 7 (**2016**), 1408.

[47]. Mondini, A., Necula-Petrareanu, G., Pauna, V.I., Iancu, L., Purcarea, C., *Cold adaptation mechanisms of Aspartate Transcarbamoylase from Glaciibacter superstes, an artic psychrophilic bacterium.* Rom. J. Biol.-Plant Biol. (**2019**), 64: 19-30.

[48]. Bosshard, H.R., Marti, D.N., Jelesarov, I., *Protein stabilization by salt bridges: concepts, experimental approaches and clarification of some misunderstandings*, J. Mol. Recognit. (**2004**), 17: 1–16.

[49]. Collins, S., E., Lasalle, V., Ferreira, M., L., *FTIR-ATR characterization of free Rhizomucor meihei lipase (RML), Lipozyme RM IM and chitosan-immobilized RML*, Journal of Molecular Catalysis B: Enzymatic, 72 (**2011**), 220-228.

[50]. Barth, A., *Infrared spectroscopy of proteins*, Biochimica et Biophysica Acta, 1767 (**2007**), 1073–1101.

[51]. Stoia, M., Istratie, R., Pacurariu, C., *Investigation of magnetite nanoparticles stability in air by thermal analysis and FTIR spectroscopy*, J Therm Anal Calorim, 125 (**2016**), 1185-1198.

ANNEX 1

The taxonomic codes corresponding to each protein sequence in each homologous microorganism, according to GenBank.

Homologs	Lipase 2_65A.3 taxid	Lipase 3 _65A.3 taxid
Psychrobacter sp. G	WP_020444543.1	WP_020442424.1
Glaciibacter superstes	WP_026851928.1	WP_022887568.1
Moritella sp. PE36	WP_043994174.1	WP_006031208.1
Escherichia coli	WP_153671715.1	WP_153670496.1
Pseudomonas aeruginosa	WP_003148542.1	WP_070333250.1
Stenotrophomonas maltophilia	WP_043400862.1	KAF1051810.1

ANNEX 2

The proportion of amino acids for each protein sequence corresponding to each microorganism homologous to the sequence of Lipase 2 from *Psychrobacter SC65A.3*.

Amino acid (%)	***Psychrobacter SC65A.3. Lipase 2***	***Glaciibacter superstes***	***Moritella sp. PE36***	***Escherichia coli***	***Pseudomonas aeruginosa***	***Stenotrophomonas maltophilia***
Ala (A)	8.3	15.0	5.6	12.7	13.4	15.6
Arg (R)	3.1	5.6	4.9	7.1	6.9	4.9
Asn (N)	4.1	1.9	3.0	0.9	0.6	1.3
Asp (D)	6.6	6.9	5.2	5.9	7.2	5.8
Cys (C)	2.1	0.3	2.0	0.6	1.9	3.2
Gln (Q)	5.2	2.2	3.6	5.6	5.0	7.5
Glu (E)	5.8	5.3	6.9	6.2	6.5	4.9
Gly (G)	6.0	9.7	8.5	8.1	7.5	8.4
His (H)	4.3	2.5	3.6	3.1	2.5	3.6
Ile (I)	6.4	3.7	6.9	1.9	2.2	2.6
Leu (L)	11.6	9.3	10.2	13.7	14.0	14.9
Lys (K)	4.8	1.2	5.6	0.9	0.9	0
Met (M)	2.3	1.9	2.0	1.6	1.9	1.3
Phe (F)	3.9	2.2	4.3	3.1	1.9	1.3
Pro (P)	5.0	6.2	5.2	5.6	6.5	7.8
Ser (S)	6.6	6.9	8.2	5.9	7.2	4.9
Thr (T)	5.8	4.7	2.6	3.7	2.5	1.9
Trp (W)	1.2	2.5	0.3	1.6	1.2	1.3
Tyr (Y)	2.3	2.8	4.9	3.7	3.4	3.2
Val (V)	4.6	9.3	6.6	8.1	6.9	5.5

The proportion of amino acids for each protein sequence corresponding to each microorganism homologous to the sequence of Lipase 2 from *Psychrobacter SC65A.3*.

Amino acid (%)	***Psychrobacter SC65A.3. Lipase 3***	***Glaciibacter superstes***	***Moritella sp. PE36***	***Escherichia coli***	***Pseudomonas aeruginosa***	***Stenotrophomonas maltophilia***
Ala (A)	9.2	10.5	9.6	7.0	11.1	9.3
Arg (R)	2.9	6.2	2.7	8.3	7.6	8.4
Asn (N)	5.4	1.4	4.8	1.3	3.2	1.6
Asp (D)	4.4	5.7	5.7	4.3	4.4	6.4
Cys (C)	0.3	0.0	0.3	2.0	0.3	0.6
Gln (Q)	3.5	0.5	3.9	6.6	4.4	4.5
Glu (E)	6.7	5.7	4.5	5.0	7.3	5.1
Gly (G)	6.3	11.0	7.2	7.6	7.0	6.1
His (H)	1.3	1.4	2.4	4.3	2.5	2.9
Ile (I)	7.6	4.3	7.8	3.3	3.5	3.5
Leu (L)	9.5	10.0	10.8	13.3	14.0	15.8
Lys (K)	8.3	1.0	3.6	2.0	2.9	1.6
Met (M)	2.2	1.9	3.6	2.7	1.9	1.6
Phe (F)	3.2	1.9	3.6	4.0	4.1	5.1
Pro (P)	4.8	8.6	7.2	5.6	7.0	7.7
Ser (S)	7.0	7.7	7.8	6.6	4.4	4.8
Thr (T)	5.4	4.8	5.1	2.3	2.2	4.2
Trp (W)	1.0	1.0	2.1	3.0	0.6	1.0
Tyr (Y)	3.5	3.3	3.0	3.0	2.5	2.9
Val (V)	7.6	12.9	4.5	7.6	8.9	6.8